

AD-A956 071



DTIC

ELECTE

NOV 22 1991

J C D

①

SAR(01)-TR-79-06
10 December 1979

91-15002



EVENT IDENTIFICATION EXPERIMENT:
PRIORITY II DATA SET

TECHNICAL REPORT NO. 6

PREPARED BY

ROBERT L. SAX, ALAN G. R. BELL, AND DONALD L. DIETZ

PREPARED FOR

AIR FORCE TECHNICAL APPLICATIONS CENTER
ALEXANDRIA, VIRGINIA 22314

ENSCO, INC.

SEISMIC APPLIED RESEARCH DIVISION
813 NORTH ROYAL STREET
ALEXANDRIA, VIRGINIA 22314

91 1104 079

CLEARED FOR OPEN PUBLICATION UNDER
THE PROVISIONS OF AFR 190-17.

JAN 15 1982

INFO SCTY BR., IG
AFTAC

79-06-80-31
0-50-81

APPROVED FOR PUBLIC RELEASE
DISTRIBUTION UNLIMITED

REPORT DOCUMENTATION PAGE		READ INSTRUCTIONS BEFORE COMPLETING FORM										
1. REPORT NUMBER SAR(01)-TR-79-06	2. GOVT ACCESSION NO.	3. RECIPIENT'S CATALOG NUMBER										
4. TITLE (and Subtitle) EVENT IDENTIFICATION EXPERIMENT: PRIORITY II DATA SET		5. TYPE OF REPORT & PERIOD COVERED Technical										
		6. PERFORMING ORG. REPORT NUMBER SAR(01)-TR-79-06										
7. AUTHOR(s) Robert L. Sax, Alan G. R. Bell, and Donald L. Dietz		8. CONTRACT OR GRANT NUMBER(s) F08606-79-C-0014										
9. PERFORMING ORGANIZATION NAME AND ADDRESS ENSCO, INC. SAR Division Alexandria, Virginia 22314		10. PROGRAM ELEMENT, PROJECT, TASK AREA & WORK UNIT NUMBERS VELA T/9705/B/PMP										
11. CONTROLLING OFFICE NAME AND ADDRESS Advanced Research Projects Agency Nuclear Monitoring Research Office Arlington, Virginia 22209		12. REPORT DATE 10 December 1979										
		13. NUMBER OF PAGES 137										
14. MONITORING AGENCY NAME & ADDRESS (if different from Controlling Office) Air Force Technical Applications Center VELA Seismological Center Alexandria, Virginia 22314		15. SECURITY CLASS. (of this report) UNCLASSIFIED										
		15a. DECLASSIFICATION/DOWNGRADING SCHEDULE										
16. DISTRIBUTION STATEMENT (of this Report) <i>Approved for Public Release. Distribution is unlimited.</i>												
17. DISTRIBUTION STATEMENT (of the abstract entered in Block 20, if different from Report)												
18. SUPPLEMENTARY NOTES ARPA Order No. 2551												
19. KEY WORDS (Continue on reverse side if necessary and identify by block number)												
<table border="0"> <tr> <td>Seismic discriminants</td> <td>Discriminant patterns</td> </tr> <tr> <td>Event identification</td> <td>Statistical learning process</td> </tr> <tr> <td>Multidiscriminant analysis</td> <td>Network performance</td> </tr> <tr> <td>Event classification</td> <td>Physical bases for discriminants</td> </tr> <tr> <td>Cluster analysis</td> <td>Signal measurements</td> </tr> </table>			Seismic discriminants	Discriminant patterns	Event identification	Statistical learning process	Multidiscriminant analysis	Network performance	Event classification	Physical bases for discriminants	Cluster analysis	Signal measurements
Seismic discriminants	Discriminant patterns											
Event identification	Statistical learning process											
Multidiscriminant analysis	Network performance											
Event classification	Physical bases for discriminants											
Cluster analysis	Signal measurements											
20. ABSTRACT (Continue on reverse side if necessary and identify by block number)												
<p>Using multidiscriminant analysis, events from a data base of 128 seismic events are identified as either earthquakes or explosions. Each event was observed by means of a network of 24 seismic stations. Discriminants derived from short-period and long-period measurements were then used to classify the events. The discriminants were based on spectral shape and on time domain measurements of event complexity. An empirical</p>												

OVER

This research was supported by the Advanced Research Projects Agency of the Department of Defense and was monitored by AFTAC/VSC, Patrick Air Force Base, FL 32925, under Contract Number F08606-79-C-0014.

AFTAC Project Number: VELA T/9705/B/PMP

Project Title: VELA Network and Automatic Processing Research

ARPA Order Number: 2551

Name of Contractor: ENSCO, Incorporated

Contract Number: F08606-79-C-0014

Effective Date of Contract: 11 December 1978

Contract Expiration Date: 31 March 1980

Project Manager: Theodore J. Cohen
(703) 548-8666

ENSCO, INC.

ii



Accession For	
NTIS GRA&I	<input checked="" type="checkbox"/>
DTIC TAB	<input type="checkbox"/>
Unannounced	<input type="checkbox"/>
Justification	
By _____	
Distribution/	
Availability Codes	
Dist	Avail and/or Special
A-1	

UNANNOUNCED

19. (continued)

Network measurements
Adaptive identification

20. (continued)

'cluster analysis' procedure was used to associate a given event with events having similar discriminant patterns. By training on known earthquakes, eight clusters were required to separate earthquakes into groups with similar discriminant patterns. Only one cluster was needed to classify explosions. These results are adaptive, in that no prior knowledge of explosion discriminant patterns were required to obtain these results. Several operational problems were identified by cluster analysis. By correcting one of these problems - magnitude scaling - and by re-running the data base, the same classification performance was obtained with only one earthquake cluster. This showed the importance of identifying and eliminating such operational problems. Our final results indicated that all of the explosions could be detected as members of a single cluster. However, 14% of the earthquakes remained unidentified and 4% were falsely identified as explosions. This evaluation neglects two explosions both of which were incorrectly edited. Additional work is needed to improve identification of earthquakes by means of multidiscriminant analysis.

SUMMARY

We processed a data base of 128 events (Priority II data set) to evaluate our baseline approach to the problem of identifying earthquakes and explosions. As was the case for all participants of the Event Identification Experiment, these data constituted a common data base of short-period and long-period seismic waveforms. The seismic signals used were recorded at fourteen single-sensor stations distributed worldwide; at three short-period and long-period array stations in Korea, the United States (Montana), and Norway; at a long-period array in Iran; and at six single-sensor stations forming a regional Alaskan network. In all, the network consisted of twenty-four seismic stations.

Our procedure for identifying these events was implemented as a system, and our goal was to emulate a practical working environment. This approach provided fast, efficient, and flexible procedures by which to identify events as earthquakes or explosions through the use of multiple discriminants. These discriminants consisted mainly of short-period and long-period measures of spectral shape and of time-domain measurements of the event complexity. Given these observations, each event was classified as follows: (1) as a member of one of the eight clusters established by training on earthquakes; (2) as a member of one or more other clusters tentatively interpreted as a possible explosion-type source; or (3) as a singular, unidentified event which simply did not cluster and could not be interpreted. It should be noted that

the adaptive clustering procedure we derived and implemented trains on earthquake data, but does not permit training on known explosion data.

As seen above, the adaptive clustering procedure used is based on the consistency of observed discriminant data. It can adaptively group events not previously encountered (e.g., events associated with unusual regional or site geological characteristics, multiple explosions, etc.). Our procedure requires detecting a pattern of four or more such unusual events before a new (anomalous) type of event can be established. It is conceivable that the discriminant pattern used for clustering an event type could be determined by training with synthetic data. In that case, the event type could be established by the observation of a single event.

With our initial, selected set of discriminants, we observed that eight discriminant clusters were needed to separate the different types of earthquakes in the data base. Some of these event clusters were found to have resulted from operational problems (i.e., problems related to our definition of discriminants and to our data processing techniques). Clustering helps to identify operational problems as well as to identify the physical factors responsible for our capability to separate explosions from earthquakes. The most important operational problem observed was that the selected event discriminants exhibited serious magnitude scaling effects. That is, the event discriminants clustered into small, medium, and large magnitude sub-groupings of a group containing deep earthquakes or of another group containing exclusively shallow earthquakes. Then, too, another earthquake

cluster probably associated with large ground-displacement overshoots was indicated by substantial high-frequency peaks in the event spectra. Unless they were clustered and treated separately, these unusual earthquakes would have been falsely classified as explosions.

A number of operational problems were identified by the adaptive clustering procedure and are discussed in detail. An attempt was made to resolve these problems, and the results obtained were encouraging.

With respect to the results obtained, one explosion in the data base was misclassified as an earthquake, and another was 'unidentified.' Post-analysis quality control checking of the data for these two events indicated that the data were not properly edited. In particular, large timing errors on the order of 30 seconds, and correspondingly large errors in magnitude measurements (one or two orders of magnitude), suggest that the data for these two events be omitted from the performance evaluation. On this basis, the following detection performance was achieved:

Explosions misidentified	0%
Explosions unidentified	0%
Earthquakes falsely identified as explosions	4%
Earthquakes which are unidentified	14%

These results indicate that a single explosion cluster effectively separates the explosions, but that improvement is needed to identify more effectively the earthquake events.

We did modify our baseline discriminants by scaling them to remove their observed dependence on network magnitudes. Using the scaled discriminants, we obtained the same partitioning of earthquakes and explosions previously obtained, but with the following difference: all of the earthquakes, which formerly fell into eight clusters, migrated into a single earthquake cluster, (the explosions still fell into a single cluster). This dramatic result indicates that the clustering previously obtained with our baseline discriminants appeared to be an artifact of the magnitude scaling problem.

The modified discriminants, empirically corrected for their dependence on network magnitude, exhibited significant differences in their ability to separate explosions from earthquakes. From this, we learned that it is important to recognize and remove operational problems before judging the efficacy of the individual discriminants. Then, too, by applying the adaptive clustering technique using the modified discriminants, it may be possible to improve event identification performance, especially by more effectively identifying earthquake events and by reducing false alarm explosion identifications.

In sum, the results we obtained in the Event Identification Experiment demonstrate the power in our clustering approach to training with earthquakes and to interpreting residual clusters (which are dissimilar to earthquake clusters) as consisting of possible explosions. Furthermore, our approach of not presuming any prior knowledge of explosion discriminant characteristics, but, instead, of relying

on clustering to provide such information, is important in that there is no 'forcing' of solutions which have limited applicability. We further learned that the recognition and solution of operational problems is essential before passing judgement on the efficacy of the discriminants. Otherwise, the interpretation of results could be misleading and lacking in generality. Clearly, then, our work indicates that much remains to be done to improve our data processing techniques before our results can be considered optimum and generally applicable.

Neither the Advanced Research Projects Agency nor the Air Force Technical Applications Center will be responsible for information contained herein which has been supplied by other organizations or contractors, and this document is subject to later revision as may be necessary. The views and conclusions presented are those of the authors and should not be interpreted as necessarily representing the official policies, either expressed or implied, of the Advanced Research Projects Agency, the Air Force Technical Applications Center, or the US Government.

ACKNOWLEDGMENTS

The authors would like to thank the following persons for their invaluable help: Robert R. Oliver, for processing the seismic events studied in this report; Jeffrey S. Shaub and David G. Black, for programming support on the PDP-15/50 computer; A. William Schmidt, Dick Mosehauer, and Leonard C. Weltman, for programming support on the IBM 360/44 computer; and Cherylann B. Saunders, for typing a difficult manuscript as expeditiously as was possible.

TABLE OF CONTENTS

SECTION	TITLE	PAGE
	SUMMARY	iii
	ACKNOWLEDGMENTS	viii
I.	EVENT IDENTIFICATION EXPERIMENT	I-1
	A. INTRODUCTION	I-1
	B. THE AREA OF INTEREST DATA BASE	I-6
	C. REPORT ORGANIZATION	I-13
II.	OVERVIEW OF THE IDENTIFICATION SYSTEM	II-1
	A. PHILOSOPHY OF EVENT IDENTIFICATION	II-1
	B. PHYSICAL BASIS FOR DISCRIMINATION	II-6
	C. CRITERIA FOR EXPLOSION IDENTIFICATION	II-9
	D. EVENT IDENTIFICATION STRATEGY	II-12
	E. RESULTS OF CLUSTER ANALYSIS	II-19
	F. OPERATIONAL PROBLEMS	II-24
III.	EVENT IDENTIFICATION SYSTEM - METHOD	III-1
	A. ACCESS SIGNAL TIME WINDOWS	III-1
	B. EXTRACT SIGNAL WAVEFORMS	III-9
	C. MEASURE SIGNALS OR NOISE	III-10
	D. SOURCE PARAMETERS ESTIMATED FROM SIGNAL MEASUREMENTS	III-22
	E. COMPUTATION OF DISCRIMINANTS	III-27
	F. CLASSIFY EVENT TYPES BY CLUSTER ANALYSIS	III-38
IV.	ABILITY OF CLUSTER ANALYSIS TO SEPARATE EARTHQUAKES AND EXPLOSIONS	IV-1

TABLE OF CONTENTS
(continued)

SECTION	TITLE	PAGE
V.	CONCLUSIONS	V-1
VI.	REFERENCES	VI-1
Appendix A	THE AUTOMATIC EDIT DETECTOR	A-1
Appendix B	VARIABLE FREQUENCY MAGNITUDE MEASURE- MENT BY A FIXED BANK OF SHORT-PERIOD AND LONG-PERIOD BANDPASS FILTERS	B-1
	A. OPTIMUM DESIGN OF BANDPASS FILTERS	B-1
	B. SAMPLING OF SPECTRAL MAGNITUDES AND MINIMIZATION OF RADIATION PATTERN EFFECTS	B-6
	C. ERROR ANALYSIS OF SPECTRAL LEAKAGE	B-8
	D. PRESENT METHOD OF FILTERED MAGNITUDE MEASUREMENT TO MINIMIZE SPECTRAL LEAKAGE ERRORS	B-12

LIST OF FIGURES

FIGURE	TITLE	PAGE
I-1	NORMALIZATION OF SKEWED DISCRIMINANTS	I-4
II-1	OUR PHILOSOPHY OF EVENT IDENTIFICATION	II-5
II-2	DISCRIMINANTS	II-8
II-3	PHYSICAL BASIS FOR DISCRIMINANTS	II-10
II-4	CRITERIA FOR EXPLOSION IDENTIFICATION	II-13
II-5	STATISTICAL LEARNING PROCESS	II-16
II-6	THRESHOLD STRATEGY FOR RELIABLY ASSOCIATING UNKNOWN EVENTS WITH ESTABLISHED CLUSTERS	II-17
II-7	THRESHOLDS FOR CLUSTERING EVENTS	II-18
II-8	PRIORITY II NETWORK PERFORMANCE BASED ON CLUSTER IDENTIFICATION	II-20
II-9	SUMMARY OF NETWORK PERFORMANCE ON THE PRIORITY II NETWORK	II-22
II-10	SCALED DISCRIMINANTS $D_I = F(m_b)$	II-26
III-1	EVENT IDENTIFICATION SYSTEM ANALYSIS PROCEDURES	III-2
III-2	DISPERSION FOR WORLD-WIDE STATIONS	III-7
III-3	PHYSICAL VALIDITY OF MAGNITUDE MEASURE- MENTS	III-14
III-4	COMPARISON OF FILTERED MAGNITUDE MEA- SUREMENTS FOR STATIONS ANMO AND I	III-17
III-5	DERIVATION OF PHASE STANDARD DEVIATION AND AVERAGE FREQUENCY OF SHORT-PERIOD P WAVES	III-20
III-6	PULSE COMPLEXITY DISCRIMINANT $f-\sigma_\phi$	III-21
III-7	MAXIMUM LIKELIHOOD ESTIMATION OF UNBIASED EVENT MAGNITUDE	III-24
III-8	PHYSICAL BASIS FOR DISCRIMINANTS	III-29
III-9	PROCEDURE FOR m_b SCALING OF DISCRIMI- NANTS	III-31
III-10	SYSTEMATIC APPROACH TO EVENT DISCRIMINA- TION	III-40

LIST OF FIGURES
(continued)

FIGURE	TITLE	PAGE
III-11	INDUCTIVE PROCEDURE FOR DETECTING ANOMALOUS EVENT GROUPS DISPLAYING CONSISTENT BUT UNKNOWN L ¹ DISCRIMINANT CHARACTERISTICS	III-42
III-12	PROCEDURE FOR ASSOCIATING NEW OBSERVATIONS WITH KNOWN CLUSTERS	III-46
IV-1	PHYSICAL AND OPERATIONAL INTERPRETATION OF THE RESULTS OF THE EIGHT EARTHQUAKE CLUSTERS	IV-2
IV-2	SEPARATION OF EXPLOSIONS	IV-4
IV-3	POPULATION PINS	IV-5
V-1	FACTORS INFLUENCING PERFORMANCE	V-3
V-2	CLASSIFICATION OF EVENTS AS EARTHQUAKES OR EXPLOSIONS	V-4
V-3	OUR PHILOSOPHY OF EVENT IDENTIFICATION	V-7
V-4	WHAT WE HAVE LEARNED	V-8
A-1	PROBABILITY OF MEASURED ENVELOPE EXCEEDING NOISE AS A ROBUST DETECTION CONCEPT FOR TIMING WEAK SIGNALS	A-3
B-1	MATHEMATICAL DERIVATION OF FILTERING PROCESS	B-2
P-2	NORMALIZATION OF SHORT-PERIOD FILTERED MAGNITUDE MEASUREMENTS	B-4
B-3	SCHEMATIC REPRESENTATION OF SHORT-PERIOD AND LONG-PERIOD FILTER COMBS	B-7
B-4	VARIABILITY OF FILTERED MAGNITUDE MEASUREMENTS	B-11
B-5	ENVELOPE AND PHASE MODULATED SIGNALS	B-14

LIST OF TABLES

TABLE	TITLE	PAGE
I-1	STATION LOCATIONS OF PRIORITY II NETWORK	I-7
I-2	EVENT PARAMETERS	I-9
III-1	EVENT IDENTIFICATION SYSTEM - SUMMARY	III-3

SECTION I
EVENT IDENTIFICATION EXPERIMENT

In this study, an experimental Event Identification System (EIS) developed by Sax, et al. (1978) was used to classify, as an earthquake or an explosion, each of 128 events drawn from an Area of Interest (AI) data base (the Priority II data set). The specific goals of the study were:

- To refine the Event Identification System developed by Sax, et al. (1978);
- To identify the 128 events as either earthquakes or explosions;
- To evaluate the performance characteristics of the Event Identification System;
- To recommend procedures for implementing the Event Identification System in an operational environment.

A. INTRODUCTION

Much research has been performed over the past two decades on the problem of seismic source identification. As a rule, event identification studies have been primarily concerned with the evaluation of one or two discriminants which were applied to data from events in specific source regions.

Often, only data from single stations or arrays, rather than from entire networks, were considered in these evaluations. Thus, these studies failed to account for variations in discriminant measurements which were introduced by differing tectonic structures beneath different source regions and different receiver locations. Also not considered were variations introduced along travel paths between different source-receiver combinations. As a result, some discriminants which were initially thought promising (such as complexity) were found to be significantly less effective when considered in light of larger data bases which encompassed different source regions and station locations. In fact, studies have suggested that even $M_s - m_b$, which has historically proven to be a powerful discriminant, should be used on a regional, rather than a global, basis (Liebermann and Pomeroy, 1969; Marshall and Basham, 1972).

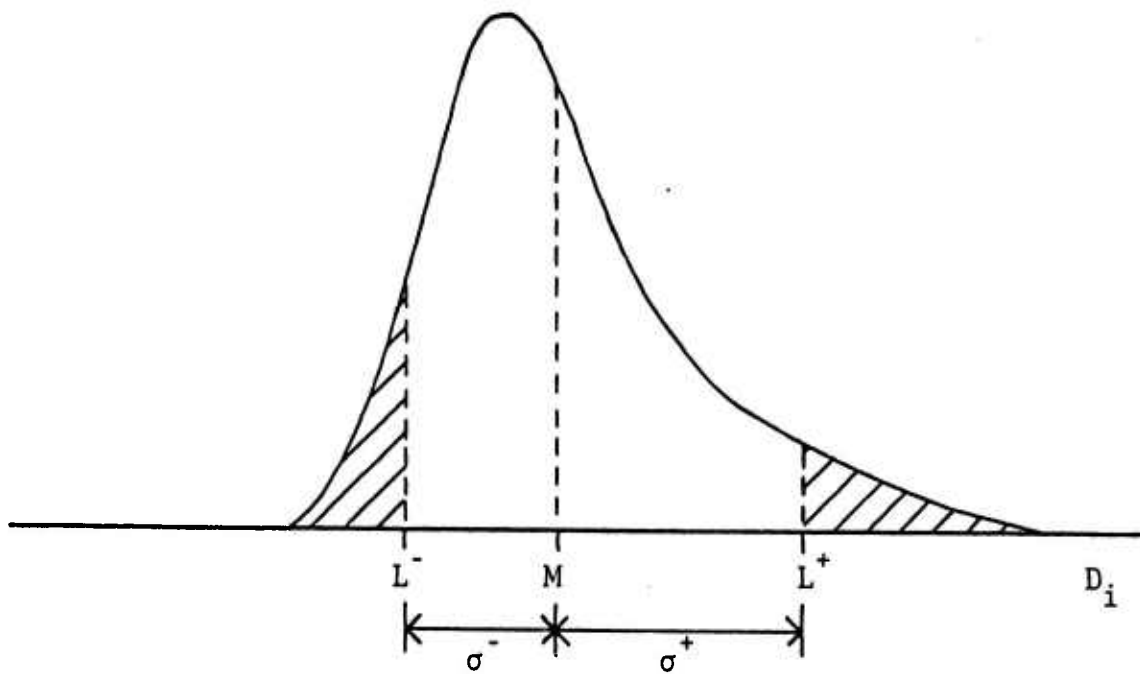
Because of the effects of source, path, and receiver variations on discriminant measurements, no single discriminant can be expected to classify correctly all events for which data are recorded by a given network of stations. For this reason, a multidiscriminant approach is taken in this study. The utility of this type of approach is demonstrated by Anglin (1971), who showed that complete separation of a suite of Eurasian earthquakes and underground explosions could be obtained using complexity and the third moment of frequency in a bivariate discrimination scheme. Individually, neither of these discriminants completely separated the two populations.

Multidiscriminant analysis (or multivariate discrimination analysis) have been studied by Booker and Mitronovas (1964) and Bell (1978). In both cases, similar techniques were used to classify, with considerable success, regional western United States earthquakes and underground explosions recorded by Long Range Seismic Measurement (LRSM) stations at a variety of different locations. Several multidiscriminant cluster analysis procedures which involve grouping events by their 'like' discrimination characteristics have been studied (Bell, 1978). They appeared promising in that event classifications derived using these procedures were entirely data motivated, and they did not require prior information in the form of event training sets.

A multidiscriminant discrimination approach was developed by Sax (1976). This approach required training on a set of earthquake and explosion data. Several important lessons were learned from that 1976 study. Some of these lessons are described below.

In Sax's 1976 study, spectral magnitude measurements were used as discriminants. These discriminants were observed to have highly skewed statistical deviations. The assumption, then, that normal statistics apply leads to sub-optimal results unless this skewed effect is taken into account.

A method was developed to transform the skewed discriminants to Z-statistics since the latter behave approximately as normal statistics. This is demonstrated in Figure I-1, wherein the discriminant D_1 is normalized by referencing



- LEVELS OF VARIATION OF DISCRIMINANT D_i
 - L_i^+ : 85% of $D_i \leq L_i^+$ 85% Level
 - M_i : 50% of $D_i \leq M$ 50% Level
 - L_i^- : 15% of $D_i \leq L_i^-$ 15% Level

- PARAMETERS FOR NORMALIZATION OF D_i
 - MEDIAN : M_i
 - POSITIVE DEVIATION: $\sigma_i^+ = |L_i^+ - M_i|$
 - NEGATIVE DEVIATION: $\sigma_i^- = |L_i^- - M_i|$

- NORMALIZATION OF D_i TO APPROXIMATE UNIT NORMAL STATISTICS

$$z_i = \frac{D_i - M_i}{\sigma_i} \quad \text{where} \quad \sigma_i = \begin{cases} \sigma_i^+ & \text{if } D_i \geq M \\ \sigma_i^- & \text{if } D_i < M \end{cases}$$

FIGURE I-1
NORMALIZATION OF SKEWED DISCRIMINANTS

observations to the median of a standard reference earthquake population. Skewness is removed by dividing the difference between the D_i and the M_i by the standard deviation of positive or negative deviations about the population median (σ_i). For multidiscriminant analyses, each component discriminant D_i of the discriminant pattern vector \underline{D} is normalized as shown in Figure I-1. Thus, for normal reference earthquakes, the normalized discriminant pattern vector \underline{Z}_N is approximately a multivariate unit normal statistic. Clustered outliers of \underline{Z}_N can be interpreted as either anomalous earthquakes or explosions.

In the 1976 study, Sax trained on eastern Kazakh and Nevada Test Site (NTS) explosions, and he obtained two normalized explosion discriminant patterns (\underline{Z}_1 and \underline{Z}_2) for the two explosion sets. Two completely different cluster models were required to identify events in the two populations. Furthermore, the correlation coefficient between these sets, $(\underline{Z}_1 \cdot \underline{Z}_2) / |\underline{Z}_1| |\underline{Z}_2|$, was 0.05; this indicated that there was no significant correlation between the normalized discriminant patterns of the two populations.

These results indicated that a serious problem conceivably existed in depending on identification criteria derived solely by training on known, central Asian explosions. Results obtained from data for NTS explosions were a case in point; here, the use of multiple discriminants derived from Asian data would have been ineffective. In fact, use of discriminants derived from central USSR events would have resulted in misidentification of NTS explosions as earthquakes. The conclusion is that in all probability, more than one

cluster model would be required to identify explosions from the two areas.

Sax, et al. (1978) developed an adaptive discrimination model as an answer to the issues raised by Sax (1976). The initial approach in the 1978 study was to assume that a single cluster could adequately represent earthquakes, but that multiple clusters would be needed to represent explosions. This strategy was successfully demonstrated by Sax, et al. (1978) using data for 35 central Asian events which were recorded at 22 world-wide stations. However, the same concept, when applied to the data for the 128 events analyzed in this report, produced unsatisfactory results. It was concluded that the negative result was due mainly to the diversity of discriminant patterns exhibited by both earthquakes and explosions. As a result, it was found necessary to change the analysis strategy to one of representing both earthquakes and explosions by means of multiple clusters, and to train on earthquake characteristics before attempting to separate explosions from earthquakes. Results shown in this report demonstrate the viability of this new identification strategy.

B. THE AREA OF INTEREST DATA BASE

The data base used in this event identification study consists of signals from 128 events drawn from the suite of 'Area of Interest' (AI) events. Event data from a network of seismic stations (listed in Table I-1) were provided by the Seismic Data Analysis Center (SDAC). The data supplied for each event generally consisted of short-period and

TABLE I-1
STATION LOCATIONS OF PRIORITY II NETWORK

Station Index	Station Designation	Latitude (°N)	Longitude (°E)	Tectonic Class*
1	BFAK	64.77	-146.89	A
2	UCAK	66.00	-153.72	A
3	TNAK	62.91	-156.02	A
4	CNAK	67.45	-144.52	A
5	ATAK	52.88	173.17	A
6	NJAK	63.06	-141.83	A
7	KSRS	37.45	127.92	I
8	NORSAR	60.84	10.89	I
9	LASA	46.69	-106.22	I
10	ILPA	35.42	50.69	A
11	HNME	46.16	-67.99	I
12	RKON	50.84	-93.67	I
13	ANMO	34.94	-98.46	R
14	ANTO	39.90	32.80	A
15	CHTO	18.79	-98.81	A
16	CTAO	-20.09	146.25	I
17	GUMO	13.59	144.87	A
18	KA AO	34.54	69.04	A
19	MA IO	36.30	59.49	A
20	MA JO	36.54	138.21	A
21	NW AO	-32.93	117.24	I
22	SH IO	25.57	91.88	A
23	TAT O	24.98	121.49	A
24	ZO BO	-16.27	-68.13	A

* A = Active, I = Inactive, R = Rift

long-period channels for each station. Seismic waveform data were provided only for those events and stations where an analyst had observed signals.

The origin times and coordinates of the events used in this study are listed in Table I-2.

In order to eliminate obvious sources of error, plots of the AI data were visually examined for mixed events and for evidence of station recording malfunctions (e.g., spikes, etc.). Data showing either of these problems were eliminated from consideration because discrimination parameters measured on these data would, in all probability, not be representative of the event.

The policy of processing data only for those stations and events for which there was an analyst-detected signal adversely affects the computation of unbiased source parameters. That is, Ringdal's maximum likelihood technique (Ringdal, 1974; 1975) was used to calculate these source parameters. Ideally, to use this technique requires the availability of either signal measurements or, if no signal was detected, of the corresponding noise measurements. Since noise data are not provided for stations and events for which there was no analyst-detected signal, it was necessary to generate a set of short- and long-period noise defaults. These noise defaults were generated for each station by averaging noise measurements from data for several events where no signal was observed. The default values are substituted for actual noise measurements for those station phases for which no data were provided (i.e., where no analyst-detected signal

TABLE I-2
EVENT PARAMETERS
(PAGE 1 OF 4)

Event Number	Date (Mo/Da/Yr)	Origin Time (Hr:Min:Sec)	Latitude ($^{\circ}$ N)	Longitude ($^{\circ}$ E)	Tectonic Class*
1	07/26/77	17:00:00	69.4	90.4	I
3	11/01/77	03:54:24	55.3	130.8	A
4	11/01/77	17:56:33	36.7	68.4	A
6	11/04/77	10:51:40	23.0	101.6	A
7	11/04/77	23:54:52	30.7	81.3	A
8	11/05/77	02:09:38	42.9	45.3	A
9	11/05/77	04:06:49	37.0	71.0	A
10	11/06/77	13:31:41	36.7	71.7	A
14	07/30/77	01:57:00	49.7	78.2	I
16	08/10/77	22:00:01	50.9	111.0	A
17	08/17/77	04:27:00	49.8	78.2	I
18	08/20/77	22:00:01	64.1	99.8	I
19	09/01/77	03:00:00	73.3	54.3	I
20	09/05/77	03:03:00	50.1	78.9	I
21	09/10/77	16:00:00	57.2	106.8	A
22	09/30/77	07:00:00	48.0	48.0	I
23	11/10/77	04:57:46	37.1	71.8	A
24	11/10/77	09:22:58	33.0	89.0	A
25	11/12/77	05:09:16	38.0	91.0	A
26	11/12/77	12:27:00	37.0	71.0	A
27	11/13/77	21:02:48	28.0	90.0	A
28	11/15/77	20:20:49	38.0	74.0	A
29	11/17/77	04:23:54	28.0	90.0	A
30	11/18/77	05:20:10	33.0	89.0	A
31	11/18/77	05:33:21	33.0	89.0	A
32	11/18/77	11:26:56	28.0	90.0	A
33	10/09/77	11:00:05	78.3	52.8	I
34	11/18/77	15:10:10	28.0	90.0	A
35	11/18/77	17:23:25	33.0	89.0	A
36	10/16/77	20:03:35	48.4	152.9	A
37	11/18/77	21:55:37	60.1	143.2	A
38	10/16/77	15:02:49	36.9	71.5	A
39	11/18/77	23:12:49	33.0	89.0	A
41	10/13/77	20:38:42	38.1	72.8	A
45	11/19/77	11:51:09	37.0	71.9	A

* A = Active, I = Inactive, R = Rift

TABLE I-2
EVENT PARAMETERS
(PAGE 2 OF 4)

Event Number	Date (Mo/Da/Yr)	Origin Time (Hr:Min:Sec)	Latitude ($^{\circ}$ N)	Longitude ($^{\circ}$ E)	Tectonic Class*
46	11/20/77	01:41:23	30.6	93.3	A
47	10/16/77	21:05:35	49.7	155.1	A
48	10/19/77	05:02:00	36.3	71.3	A
49	10/19/77	21:20:37	49.5	155.4	A
50	10/20/77	08:18:04	56.3	164.1	A
53	10/29/77	03:07:00	49.8	78.0	I
55	10/26/77	05:38:52	49.0	155.8	A
56	10/26/77	07:11:31	46.4	153.5	A
57	10/26/77	13:14:31	51.5	153.4	A
58	10/27/77	07:20:29	53.5	160.0	A
59	10/28/77	21:15:12	39.8	71.9	A
60	10/29/77	04:14:56	47.0	152.3	A
61	10/29/77	06:26:42	41.0	63.7	A
62	10/29/77	10:33:59	47.3	153.1	A
63	10/30/77	21:38:16	44.8	145.0	A
64	10/31/77	09:40:04	55.8	162.7	A
65	11/20/77	11:01:22	56.8	108.5	A
66	11/20/77	18:55:28	39.9	73.9	A
67	11/20/77	20:57:24	38.0	72.2	A
68	11/20/77	23:40:35	33.1	88.1	A
69	11/21/77	19:43:36	36.4	71.1	A
70	11/22/77	00:07:49	37.0	71.0	A
72	11/22/77	06:56:13	36.2	70.8	A
73	11/22/77	11:33:45	43.0	89.0	A
74	11/22/77	19:16:12	40.0	75.0	A
75	11/23/77	10:28:07	34.0	83.0	A
76	11/26/77	15:44:41	37.0	71.0	A
77	11/26/77	22:46:46	37.0	115.0	A
78	11/27/77	02:09:07	28.0	90.0	A
79	11/27/77	03:57:00	50.0	79.0	I
80	11/28/77	09:02:26	43.2	47.6	A
81	11/30/77	04:06:59	49.9	78.8	I
143	12/02/77	12:57:10	52.9	159.7	A
144	12/02/77	16:15:34	46.1	144.9	A
145	12/03/77	17:06:21	41.9	131.1	A

* A = Active,

I = Inactive,

R = Rift

TABLE I-2
EVENT PARAMETERS
(PAGE 3 OF 4)

Event Number	Date (Mo/Da/Yr)	Origin Time (Hr:Min:Sec)	Latitude (^o N)	Longitude (^o E)	Tectonic Class*
146	12/04/77	04:03:47	56.2	163.1	A
147	12/04/77	11:39:02	48.2	146.5	A
148	12/05/77	23:37:32	55.3	162.0	A
149	12/06/77	10:52:53	41.4	69.7	A
150	12/07/77	02:03:37	41.0	72.0	A
151	12/07/77	16:19:33	35.6	94.5	A
152	12/08/77	02:02:54	52.9	89.7	A
153	12/08/77	06:45:20	41.0	72.0	A
154	12/08/77	13:57:04	50.4	149.8	A
155	12/08/77	23:37:22	36.2	70.5	A
156	12/09/77	04:23:36	54.4	160.6	A
157	12/10/77	21:58:51	51.3	156.5	A
158	12/12/77	11:06:42	51.4	157.5	A
159	12/13/77	06:58:59	35.4	88.4	A
160	12/13/77	11:34:20	42.3	133.2	I
161	12/15/77	05:15:45	36.4	70.9	A
162	12/15/77	15:07:51	43.2	45.1	A
163	12/15/77	15:23:30	43.6	45.3	A
164	12/16/77	07:11:41	43.2	146.7	A
165	12/16/77	09:08:59	51.6	159.4	A
166	12/16/77	10:15:27	33.3	97.5	A
167	12/16/77	17:55:14	36.8	59.7	A
168	12/16/77	23:17:17	43.0	47.0	A
169	12/18/77	06:57:33	55.2	160.5	A
170	12/18/77	16:47:17	39.8	77.3	A
171	12/18/77	19:09:21	51.1	157.8	A
172	12/18/77	20:43:05	39.7	77.6	A
173	12/19/77	18:12:25	39.7	77.7	A
175	12/20/77	07:27:38	39.7	69.3	A
176	12/20/77	20:52:10	55.7	158.2	A
177	12/21/77	08:30:46	41.9	47.9	A
178	12/21/77	16:39:33	52.9	159.8	A
179	12/21/77	20:17:13	36.1	68.6	A
180	12/21/77	20:40:05	52.8	159.5	A
182	12/22/77	14:05:45	52.9	159.9	A

* A = Active, I = Inactive, R = Rift

TABLE I-2
EVENT PARAMETERS
(PAGE 4 OF 4)

Event Number	Date (Mo/Da/Yr)	Origin Time (Hr:Min:Sec)	Latitude (°N)	Longitude (°E)	Tectonic Class*
183	12/22/77	19:34:05	53.1	163.4	A
184	12/23/77	07:31:44	44.8	32.8	A
185	12/23/77	09:09:54	39.5	77.4	A
186	12/24/77	03:27:52	51.2	156.9	A
187	12/25/77	08:33:37	50.0	91.0	A
188	12/25/77	17:38:42	40.9	69.7	A
189	12/26/77	04:02:57	49.8	78.1	I
190	12/26/77	05:15:21	39.9	71.9	A
191	12/26/77	23:04:34	33.7	80.8	A
192	12/27/77	07:10:11	28.0	90.0	A
193	12/27/77	12:31:00	54.7	161.5	A
194	12/28/77	15:10:46	56.0	162.0	A
195	12/31/77	03:24:38	39.1	91.1	A
264	03/20/76	04:03:45	50.0	77.0	I
265	03/29/77	03:57:00	50.0	78.0	I
266	03/19/78	03:47:00	50.0	78.0	I
267	06/11/78	02:57:00	50.0	79.0	I
268	07/28/78	02:47:00	50.0	78.0	I
269	08/09/78	18:00:00	64.0	125.0	I
270	08/24/78	18:00:00	66.0	112.0	I
271	08/29/78	02:37:00	50.0	78.0	I
272	09/05/78	00:22:00	43.0	89.0	I
273	09/21/78	15:00:00	66.0	86.0	I

* A = Active, I = Inactive, R = Rift

was observed). This approach assumes one-hundred percent operational reliability and seismic noise stationarity at each station. Because at some stations the noise field tends to be unstable, the unbiased magnitude estimates may not be accurate. However, where the above assumptions are valid, the estimates should provide reasonable estimates of unbiased event magnitudes.

C. REPORT ORGANIZATION

The organization of this report is as follows. Section II provides an overview and executive summary of our results of the Event Identification Experiment. Section III provides a description of the methodology followed in performing event discrimination, the problems encountered and some recommendations for dealing with those problems. Section IV provides a more detailed discussion of the results of cluster analysis of discriminants. The performance of individual discriminants is described in detail. Section V briefly describes conclusions drawn from this study. Section VI is a list of references. Appendix A provides a detailed description of an automatic detector used to edit event waveforms. Appendix B describes the filtering process required to effectively measure variable frequency magnitudes of seismic signals.

SECTION II

OVERVIEW OF THE IDENTIFICATION SYSTEM

The following is a general discussion of our work on event identification. The topics covered include our philosophy (or guiding principles); the physical basis of selecting discriminants; criteria for associating discrimination measurements with explosions; strategy for performing event identification; results of the event identification process; and a brief description of our systems approach to performing event identification processing.

A. PHILOSOPHY OF EVENT IDENTIFICATION

A set of guiding principles underlies our approach to event identification. The data upon which identification decisions are based are patterns, or clusters, of discriminant measurements. These patterns are designed to convey information about the source which is as independent as is possible of path and receiver effects. Also minimized are radiation pattern effects associated with the orientation of source dislocations. Basic source mechanisms (such as shear faults, tensile faults, adiabatic phase changes, explosions, and combinations of the above failure modes) are expected to result in discriminant patterns which uniquely characterize a seismic source. Source environmental factors also affect the clustering and variance of observed discriminants. These factors include shear, tensile, and compressive

strength of the medium and medium homogeneity; elasticity; associated structural geology and plate tectonics; and rheological properties of the inelastic medium. Dynamic source factors, too, influence the observed discriminant characteristics. These involve the motion and growth of source dislocations; stick-slip, elastic rebound and other mechanisms which complicate the source time function; and complex spatial patterns of fracture and dislocation occurring after the initial failure of the medium.

Given the immense complexity of the event identification problem, it is unlikely that any single discriminant will suffice to identify and separate effectively all types of earthquakes and explosions; it is expected that multiple discriminants will be needed to do that. The determination of what discriminants should be used for this purpose, however, is an evolutionary process, and such a determination is considered by us to be one of the most important goals of the Event Identification Experiment. In order to achieve the most effective monitoring of explosions by seismic means, it is essential to develop a complete set of discriminants to map uniquely all discriminant patterns into source characterizations which encompass all types of earthquakes and explosions. In short, all types of earthquakes and explosions should generate distinguishable discriminant patterns. Conversely, it should be possible to associate observed discriminant patterns with models characterizing earthquakes or explosions. Ideally, the discriminants required for homomorphic transformations of discriminants to designated source models will be generalized and improved by physical source characterization studies. Unfortunately, we are not yet to the point where this is

feasible, and so, we must depend in large part on adaptive, empirical methods for characterizing earthquakes and explosions.

In short, our approach to the event identification problem is to define a set of discriminants which are based on spectral shape and on time-domain measures of source and coda complexity; to determine stable discriminant clusters by training intensively on earthquakes; and, either operationally or physically, to characterize event groupings determined by cluster analysis or to discard them. Clusters characterized by operational problems will 'feed back' on our procedures of measuring signals and defining discriminants. Through the application of corrective procedures, event groupings indicative of operational problems will disappear as the problems are identified, corrected, and eliminated. Ultimately, we will isolate groupings of events which exhibit significant, 'like' physical characteristics.

This approach to discrimination implies a need for flexibility in altering our basis for performing event identification. Cluster analysis enables us to sort through large data bases and, adaptively, to find and estimate models which accurately characterize a subset of events in the data base. The implication here is that any single event observation can be rapidly associated with formerly observed clusters of event discriminants. Importantly, unknown types of events can be adaptively identified by the clustering of at least four events (the number of events which, by our definition, is required to statistically define a new cluster). Note, in passing, that this adaptive approach makes evasion difficult.

This is so because cluster analysis automatically trains on the discriminant pattern emitted by a new source type, and will isolate those events exhibiting characteristics different from events previously observed.

Another benefit of cluster analysis is that it rapidly defines operational problems. For example, if events cluster by magnitude, a magnitude scaling problem is indicated. Should this occur, our linearly programmed system for generating and maintaining data base file structures, and our programmable interactive capability, provide for the rapid scaling of the discriminants. Once done, the data base can quickly be rerun, and the files can immediately be updated as a normal operating procedure.

Another example of our system analysis approach relates to clustering station measurements of source parameters. Suppose, for example, that discriminant clusters observed at a station are associated with event distance, or even with particular source regions. In such cases, the operational problem is one of correcting magnitudes properly with distance, or, possibly, one of providing source-region-to-station corrections for magnitude. Cluster analysis provides a means of determining rapidly whether such problems exist. Further, the speed with which such operational problems can be defined and corrected through the use of a systems approach is one of the principal lessons to be learned from the Event Identification Experiment.

A summary of our philosophy of event identification is shown in Figure II-1.

FIGURE II-1
OUR PHILOSOPHY OF EVENT IDENTIFICATION

- SIMILAR SOURCE MECHANISMS SHOULD YIELD SIMILAR DISCRIMINANT PATTERNS
- THE DISCRIMINANT SET WILL EVOLVE TO ENCOMPASS ALL TYPES OF EARTHQUAKES AND EXPLOSIONS
- STABLE EVENT CLUSTERS DETECTED EMPIRICALLY MUST BE PHYSICALLY OR OPERATIONALLY CHARACTERIZED, OR THEY MUST BE DISCARDED
- DISCRIMINANTS SHOULD BE GENERALIZED AND IMPROVED UPON BY PHYSICAL SOURCE STUDIES
- PRACTICAL IDENTIFICATION PROCEDURES WHICH ARE DEVELOPED SHOULD BE IMPLEMENTABLE ON A REAL-TIME SYSTEM
- A SYSTEMS APPROACH WILL BE APPLIED TO IDENTIFICATION IN ORDER TO SPEED THE LEARNING PROCESS, TO PROVIDE FOR FLEXIBLE ANALYSIS, AND TO EASE DATA BASE MAINTENANCE REQUIREMENTS.

B. PHYSICAL BASIS FOR DISCRIMINATION

One of the most difficult decisions to be made in the course of this experiment was that of selecting a set of discriminants which would effectively separate explosions from earthquakes. Two considerations went into the selection. One consideration was that the discriminant set had to include as many obvious physical differences between explosions and earthquakes as was possible. The other consideration was to recognize that discriminant measurements are subject to large random variations, due, simply, to the complexity of the earth. Note that some redundancy in the discriminants selected is considered necessary to cover effectively all of the physical bases for separating explosions from earthquakes.

Given the considerations above, eighteen discriminants were initially selected for use in the experiment. An obvious issue to be raised with this approach, however, is that of avoiding the accumulation of large errors which are associated with weaker discriminants. These large, random deviations would tend to mask the effect of the better discriminants. This problem was resolved here by employing a weighting scheme for gauging the similarity of discriminant patterns. This procedure is described later in this report in detailed derivations of the cluster analysis procedures. The net effect of the weighting procedure now in place is to reduce the 'effective size' of the discriminant set such that it yields smaller random deviations expected from only a few normalized discriminants. We believe that this procedure provides an effective basis for operating with large discriminant sets, but

with little degradation in the effectiveness of the better discriminants. Nonetheless, as we learn to operate with large discriminant sets, we will eliminate those which prove to be less effective; we will also add discriminants which prove to be more effective in separating explosions from earthquakes and in stabilizing the cluster analysis of events.

The physical bases for selecting discriminants relate to (shallow) depth; to the efficient generation of compressional waves; to smaller, higher-stress and full, stress-drop sources; to elastic rebounded or resonant sources; to lower backscattering from smaller, shallow sources; to less complex, first motion of the source-time function; and to combinations of the preceding effects. A list of the selected discriminants is shown in Figure II-2.

M_s is defined as narrowband-filtered ground displacement magnitudes averaged at four periods (see Legend, Figure II-2). This definition differs from the conventional definition in that amplitude measurements are not divided by the period. As a result, long-period surface wave magnitudes computed here are relatively constant over frequency, and are comparable in value to short-period m_b determination. The average period of M_s , as defined here, is 24 seconds. Discriminants D_1 , D_2 , and D_5 (shown in Figure II-2) are differences of surface wave ground displacement magnitudes between 50 seconds and 14 seconds period, while discriminants D_3 , D_4 , and D_{11} are slopes of compressional wave ground displacement magnitudes between 0.3 and 1.3 Hz. Discriminants D_6 , D_7 , and D_8 are measures of compressional wave energy for a given moment source as indicated by network m_b relative to long-period surface waves or compressional waves. The scaling of D_6 is

FIGURE II-2
DISCRIMINANTS

$$\begin{aligned}
 D_1 &= M_s - M_s(50) \\
 D_2 &= M_s(14) - M_s \\
 D_3 &= [m_b(0.5) - m_b(0.3)]/0.2 \\
 D_4 &= [m_b(0.8) - m_b(0.5)]/0.2 \\
 D_5 &= M_s(14) - M_s(17) \\
 D_6 &= 1.14m_b - M_s - 1.79 & m_b \leq 4.9 \\
 &= 1.55m_b - M_s - 3.79 & m_b > 4.9 \\
 D_7 &= m_b - M_s(50) \\
 D_8 &= m_b - m_b(0.3) \\
 D_9 &= m_b(3.2) - m_b(0.3) \\
 D_{10} &= \bar{f} - \bar{\sigma}_\phi \text{ (pulse complexity)} \\
 D_{11} &= [m_b(1.3) - m_b(0.8)]/0.2 \\
 D_{12} &= [m_b(2.0) - m_b(0.5)]/0.6 \\
 D_{13} &= \text{Min}\{ \int_0^5 f^5 A^2 dt / \int_5^{10} f^{10} A^2 dt \} \text{ (coda complexity)} \\
 D_{14} &= D_{12} + D_6 \\
 D_{15} &= 3D_{10} + D_{11} \\
 D_{16} &= 3D_{10} + D_6 \\
 D_{17} &= 3D_{10} + D_9 \\
 D_{18} &= 3D_{10} + D_{12}
 \end{aligned}$$

LEGEND

- D_i = The i^{th} discriminant
 m_b = Network bodywave magnitude
 M_s = $(M_s(33) + M_s(25) + M_s(20) + M_s(17))/4$
 $M_s(T)$ = Narrowband-filtered surface waves of period T sec
 $m_b(f)$ = Narrowband-filtered P-waves of frequency f Hz
 \bar{f} = Average frequency of first 1.5 sec of P-wave pulse
 $\bar{\sigma}_\phi$ = Phase standard deviation of first 1.5 sec of P-wave pulse
 $A(t)$ = Amplitude-time variation.

taken from the result of Strauss (1978) for unbiased M_s - versus- m_b at the Alaskan Long Period Array (ALPA). Discriminants D_9 and D_{12} are frequency-dependent magnitude discriminants designed to identify small, full stress-drop events (see Bache, et al., 1974; Archambeau, 1978, 1979, personal communications). Discriminants D_{10} and D_{13} are time-domain complexity measures, while D_{13} is a short-time-gate, minimum-coda-complexity measure; this discriminant is designed to take advantage of the smaller backscattering associated with small, shallow-focus sources (this reflects on the normally large, scattering attenuation in shallow crustal layers). Discriminant D_{14} is based on the linear relationship which has been observed between average frequency and average standard deviation of phase angle versus time-of-first-motion ground acceleration (see Unger, 1978). Note that D_{14} is interpreted as an alternative measure of small, high-stress or full stress-drop sources, as indicated by the higher-frequency signatures and the simpler first-motion of such sources. Discriminants D_{14} through D_{18} are 'combined effect' discriminants which are based on the observed behavior of discriminant pairs. Figure II-3 associates the selected discriminants with various physical mechanisms.

C. CRITERIA FOR EXPLOSION IDENTIFICATION

As indicated above, we are concerned that explosions be identifiable without prior knowledge of the discriminant pattern. For example, shot arrays from some unknown, tectonically active region could conceivably emit a multiple discriminant pattern which is totally different from that of

FIGURE II-3
PHYSICAL BASIS FOR DISCRIMINANTS

- SHORTER PERIOD SURFACE WAVES AND RISE IN LOW FREQUENCY P-WAVE SPECTRUM DUE TO SHALLOW DEPTH

$D_1 = M_s - M_s(50)$	$D_3 = m_b(0.5) - m_b(0.3)$
$D_2 = M_s(14) - M_s$	$D_4 = m_b(0.8) - m_b(0.5)$
$D_5 = M_s(14) - M_s(17)$	$D_{10} = \bar{F} - \bar{\sigma}_\phi$
- MORE EFFICIENT PRODUCTION OF P-WAVES AND LESS EFFICIENT PRODUCTION OF SHEAR WAVES

$D_6 = m_b - M_s$	$D_8 = m_b - m_b(0.3)$
$D_7 = m_b - M_s(50)$	
- SMALL, HIGH-STRESS AND FULL STRESS-DROP SOURCES

$D_{12} = m_b(2.0) - m_b(0.5)$	$D_{10} = \bar{F} - \bar{\sigma}_\phi$
$D_9 = m_b(3.0) - m_b(0.3)$	
- ELASTIC REBOUND OF SOURCE LEADING TO OVERSHOOT OF THE DISPLACEMENT PULSE AND TO ROLL-UP OF THE HIGH FREQUENCY SPECTRUM

$D_4 = m_b(0.8) - m_b(0.5)$	$D_{12} = m_b(2.0) - m_b(0.5)$
$D_{11} = m_b(1.3) - m_b(0.8)$	$D_9 = m_b(3.0) - m_b(0.3)$
- LESS BACKSCATTER FROM SMALLER, SHALLOW SOURCE OR LESS COMPLEX SOURCE

$D_{13} = \text{Coda Complexity}$
 $D_{10} = \text{Pulse Complexity } \bar{F} - \bar{\sigma}_\phi$
- COMBINED EFFECTS

$D_{14} = D_{12} + D_6$	$D_{17} = 3D_{10} + D_9$
$D_{15} = 3D_{10} + D_{11}$	$D_{18} = 3D_{10} + D_{12}$
$D_{16} = 3D_{10} + D_6$	

known explosions. The system designed to detect explosions, therefore, must adaptively associate these 'new type' events by cluster analysis, and label them as being different from other known types of explosions or earthquakes.

In the case of anomalous explosions the discriminants used to identify and distinguish such events from other types of events must, through training, be a complete description of explosions. In like manner, prior training on earthquakes must be intensive enough to distinguish all conceivable types of earthquake sources. Thus, if such a 'new type' cluster of events is detected in an area, and the depth range suggests that the events are explosions, the area can then be put under surveillance as a possible nuclear test site. By definition, at least four events are required here to identify an anomalous cluster of events; however, it is estimated that a cluster of from six to eight events would be required before identification of a new class of events is made by our adaptive identification procedure. It should be pointed out, however, that simulations of evasion scenarios could be prepared to establish cluster patterns for the discriminants used. In such cases, only one 'event,' or at most a few such 'events,' would be required for the cluster pattern to be established.

One serious problem which exists in addressing the event identification problem is related to the uniqueness of any identification which is made. The question may be posed as to whether unknown explosion environments exist which yield completely different discriminant patterns from those associated with known explosion environments. Experience gained by comparing eastern Kazakh events to Nevada Test Site

events points to the existence of such unknown environments. It may further be asked: How many such environments, yielding distinguishable discriminant patterns, exist? At this time, there is no way of knowing. Thus, until we reach the state where discriminant patterns can be accurately predicted and simulated on a theoretical basis from known geological and geophysical parameters, it appears that an adaptive discrimination capability will be needed for event identification. Even if such discriminant patterns are unknown, the adaptive discrimination capability developed here will increase significantly an adversary's risk in testing more than four events from a new site. The use of the adaptive discrimination capability, therefore, is a necessary adjunct to an on-line discrimination capability.

A summary of criteria for explosion identification is given in Figure II-4.

D. EVENT IDENTIFICATION STRATEGY

The first step in the identification process is to 'train' on known earthquake data from a specified geographical area with the intent being to define cluster models which characterize the earthquakes. That is, all of the known earthquakes are placed in an initial training set. For this training set, medians and standard deviations for each discriminant are obtained, as is outlined in Figure I-1. Next, our adaptive Anomalous Event Detector (AED) searches for sets of events which have similar discriminant patterns, but which are outliers of the training set. If at least four events

FIGURE II-4
CRITERIA FOR EXPLOSION IDENTIFICATION

- NO PRIOR KNOWLEDGE REQUIRED OF EXPLOSION DISCRIMINANT PATTERNS
- NO PRIOR KNOWLEDGE REQUIRED OF THE NUMBER OF PATTERNS REQUIRED TO IDENTIFY UNIQUELY ALL EXPLOSION TYPES
- ALMOST ALL EARTHQUAKE DISCRIMINATION PATTERNS ARE ASCERTAINABLE BY INTENSIVE TRAINING ON EARTHQUAKES
- 'NEW TYPE' EVENTS ARE ASSOCIATED WITH ONE ANOTHER BY ADAPTIVELY DETECTING UNKNOWN, BUT SIMILAR, DISCRIMINANT PATTERNS
- 'NEW TYPE' EVENT CLUSTERS ARE OPERATIONALLY TREATED AS 'POSSIBLE EXPLOSIONS' UNTIL PROVEN OTHERWISE
- CLUSTERED EVENT TYPES MUST BE DESCRIBED AND INTERPRETED PHYSICALLY (i.e., THEY MUST HAVE RATIONAL, PHYSICAL BASES FOR CLUSTERING).

are detected in one of the outlier sets, these events are grouped as a cluster; three or less outlier events will remain in a buffer as 'unidentified events.' This procedure is continued until the initial training set of earthquakes is clustered (unclustered outliers are retained as 'unidentified events'). As a result of the process, each cluster of earthquakes now constitutes a new training set of events from which medians and standard deviations of each cluster can be determined. Thus, after initializing the clusters required to define earthquakes, an entire data base can be processed with the intent being to identify as many events as possible as either earthquakes or explosions.

To separate explosions from earthquakes, a two-step process is used. Correlation thresholds are set on each earthquake cluster based on stability criteria. Acceptance thresholds are set as high as possible to identify unknown events, but low enough to keep cross-talk (jumps from one cluster to another) at an acceptable level. The first step of the process involves the identification of obvious earthquakes by their association with an established earthquake cluster. These identified earthquakes are then removed from the queue of unidentified events. The second step applies an Anomalous Event Detector to search for new clusters. Events in these clusters are designated as possible explosions.

Cluster analysis sifts and associates event descriptor information out of a large data base. The results depend on the search strategy employed. Decision thresholds associate unknown events with a previously observed discriminant

pattern. This, obviously, is an empirical, statistical learning process (Figure II-5). It is important, therefore, to understand, either operationally or physically, why events cluster. If clusters are associated with operational problems, then the problem should be resolved. Examples of operational problems include clustering of events having few detections; clustering of events by magnitude; etc. On the other hand, if clusters are associated with physical factors, then such factors are established as statistically significant observations. Examples of physical factors include associations with event depth; high-frequency P-wave peaks (indicating overshoot); anomalously high P-wave amplitudes; etc. Only clusters based on physical characterizations can be expected to provide meaningful identification results.

In the course of the Event Identification Experiment, a threshold strategy was pursued to reliably associate known events with established event clusters. The established clusters consisted of event groupings which were obtained by training intensively on the earthquake discriminant data. Our identification and threshold strategy employing a cluster analysis is summarized in Figure II-6.

Training on earthquakes produced eight earthquake clusters. The optimum thresholds determined for use in cluster association are shown in Figure II-7. Observation errors of cluster association are reduced to unit normal Z-statistics as gauged by the difference between observed discriminants and median discriminants, divided by the standard deviation (this procedure was described earlier in Figure I-1). Errors less than one standard deviation are weighted zero (0);

FIGURE II-5
STATISTICAL LEARNING PROCESS

- TRAIN ON EARTHQUAKES
- ASSOCIATE UNKNOWN EVENTS TO ESTABLISHED CLUSTERS
- IDENTIFY REMAINING UNKNOWN EVENT TYPES BY ADAPTIVELY DETECTING NEW CLUSTERS
- INTERPRET THE CLUSTERED EVENT GROUPS
 - PHYSICAL CHARACTERIZATIONS
 - REGIONAL ASSOCIATION
 - OPERATIONAL PROBLEMS

FIGURE II-6
THRESHOLD STRATEGY FOR RELIABLY ASSOCIATING
UNKNOWN EVENTS WITH ESTABLISHED CLUSTERS

- SET HIGH ACCEPTANCE LEVEL FOR STABLE CLUSTERS
- SET LOW ACCEPTANCE LEVEL FOR UNSTABLE CLUSTERS
- TEST THE STABILITY OF THRESHOLD CHANGES
- CONSTRAIN THRESHOLD SETTING TO ASSURE LOW FALSE-ALARM RATE

FIGURE II-7
THRESHOLDS FOR CLUSTERING EVENTS

	Cluster	Threshold*	Predicted Percent Associated**	Predicted Likelihood Ratio***
Stage I	EQ-1	0.84	60%	1.5
	EQ-2	0.97	67%	2.0
	EQ-3	0.84	60%	1.5
	EQ-4	0.84	60%	1.5
	EQ-5	0.63	47%	0.9
Stage II	EQ-6	0.84	60%	1.5
	EQ-7	0.84	60%	1.5
	EQ-8	0.60	45%	0.8
	EX-1	1.63	87%	6.7

* Deviations from the cluster median in standard deviations; normalized as shown in Figure I-1

** Based on unit normal statistics, positive and negative deviations less than the indicated threshold

*** Based on unit normal statistics, ratio of capture probability to miss probability for indicated cluster population.

larger, one (1). As previously described, this weighting scheme is designed to reduce the accumulation of errors which are usually associated with the less effective discriminants. Based on unit normal statistics, Figure II-7 shows the percentage of unknown events which can be correctly associated with a cluster. That is, this percentage of events is expected to be correctly identified. The likelihood ratio for correct identification is also shown as the ratio of 'captures' to misses. Percentage captures close to 100%, and large likelihood ratios, are indicators of stable cluster identification.

With respect to event identification, two steps were involved. First, identifications as earthquakes were based on application of the first twelve discriminants. Then, the full set of eighteen discriminants was applied to analyze further earthquake clusters EQ-6 through EQ-8. The Anomalous Event Detector (AED) was applied to the remaining set of unknown events, and this resulted in the detection of the explosion cluster EX-1. The remaining, unassociated events were assigned 'unidentified' status.

E. RESULTS OF CLUSTER ANALYSIS

Cluster identifications are based on the thresholds shown in Figure II-7; these identifications are shown in Figure II-8. The analysis was performed on a data base of 128 events, 22 of which are believed to be explosions. With regard to explosions, only one decision error was made. Specifically, one explosion was incorrectly associated with

FIGURE II-8
 PRIORITY II NETWORK PERFORMANCE BASED ON
 CLUSTER IDENTIFICATION

Event Number Decision	Event Number Decision	Event Number Decision	Event Number Decision
1 X1	39 Q5	79 U	172 U
3 Q4	41 Q3	80 U	173 Q2
4 Q1	45 Q5	81 X1	175 Q6
6 Q7	46 Q2	143 Q5	176 Q1
7 Q7	47 U	144 Q3	177 U
8 U	48 Q3	145 Q2	178 Q8
9 Q3	49 Q6	146 Q5	179 Q6
10 Q2	50 Q6	147 Q3	180 Q1
14 X1	53 X1	148 Q3	*182 X1
16 X1	55 Q2	149 Q6	183 Q1
17 X1	56 Q1	150 Q2	184 Q3
18 X1	57 Q5	151 Q1	*185 X1
19 X1	58 Q3	152 Q7	186 U
20 X1	59 Q7	153 Q1	187 Q2
21 X1	60 Q2	154 Q3	188 Q2
22 X1	61 Q2	155 U	189 X1
23 Q2	62 Q1	156 Q1	190 Q1
24 Q5	*63 X1	157 Q5	191 Q2
25 Q5	64 U	158 Q5	192 Q2
26 Q2	65 U	159 Q2	193 Q5
27 Q7	66 Q2	160 Q2	194 Q2
28 Q7	67 Q7	161 Q2	195 Q6
29 Q2	68 Q5	162 Q8	264 Q3
30 U	*69 X1	163 Q6	265 X1
31 Q6	70 Q7	164 Q6	266 X1
32 Q6	72 Q7	165 Q7	267 X1
*33 Q5	73 Q8	166 U	268 X1
34 Q2	74 Q7	167 Q2	269 X1
35 Q7	75 U	168 Q2	270 X1
36 Q7	76 Q7	169 Q4	271 X1
37 Q4	77 Q1	170 U	272 U
38 Q3	78 U	171 Q4	273 X1

LEGEND: * Decision Error
 U Unidentified Earthquake
 Q_j..... jth Earthquake Cluster
 X_j..... jth Explosion Cluster

earthquake cluster EQ-5, which is associated with a group including deep events and which had few, if any, detected signals. Figure II-9 summarizes the network performance for the Priority II data set. The observed identification of 91% of the explosions corresponds closely to the 87% identification level predicted from normal statistics (Figure II-7). Of the explosions not identified as explosions, one was classified as 'unidentified' and one was missed (i.e., false identified as an earthquake).

An alternative performance evaluation can be given which omits events #33 and #79. The data for both of these events probably contain editing errors. Event #33 was apparently detected at three stations with travel-time residuals between 20 and 30 seconds. At NORSAR, it was detected with a P-wave magnitude deviation of +1.0. Event #79 had an apparent short-period signal detected at ILPA. Using this signal, however, the event is computed to occur 37 seconds late with a P-wave magnitude error of +1.7 magnitude units. Neglecting these two events, the network performance was as follows:

- Explosions correctly identified 100%
- Earthquakes correctly identified 82%.

Of the 18% of the earthquakes not correctly identified, 14% were unidentified and 4% were false alarm explosions.

The results above are considered a baseline from which improved discrimination procedures can be gauged. Further, implementation of the following procedures should procure a significant improvement in event discrimination performance:

FIGURE II-9
 SUMMARY OF NETWORK PERFORMANCE FOR
 THE PRIORITY II NETWORK

	Number	Percent
• IDENTIFIED EXPLOSIONS	20	91
• UNIDENTIFIED EXPLOSIONS	1	5
• MISSED EXPLOSIONS	1	5
• IDENTIFIED EARTHQUAKES	87	82
• UNIDENTIFIED EARTHQUAKES	15	14
• MISSED EARTHQUAKES (FALSE ALARM EXPLOSIONS)	4	4
{ Total number of earthquakes = 106 } { Total number of explosions = 22 } { Total number of events = 128 }		

- Improve signal and event measurement techniques.
- Properly scale the discriminants for event magnitude.
- Train on earthquakes with properly scaled discriminants.

Cluster analysis represents a significant step forward in the use of multiple discriminants for identification purposes. In the case of this experiment, the partitioning of earthquakes into clusters produced the following results:

- Events in clusters EQ-1, EQ-2, EQ-5, EQ-6, and EQ-8 are predominantly shallow earthquakes.
- Events in clusters EQ-3 and EQ-7 are associated with deep earthquakes.
- Events in cluster EQ-4 are anomalous, shallow earthquakes which are explosion-like in that they exhibit enhanced, high-frequency compressional waves.
- The median magnitude m_b of cluster EQ-5 is 4.1; of cluster EQ-6, 4.9; and of cluster EQ-8, 5.3.

With respect to the last result above, an operational problem is evidenced by the partitioning by magnitude; that is, the discriminants need to be scaled with magnitude to more effectively and reliably separate earthquakes and explosions. To some extent, the clustering of events with no detected signals in cluster EQ-5 indicates another operational problem. Here, the results suggest that the procedure used for estimating unbiased magnitudes is underestimating the

spectral magnitudes of events with few detections. This procedure needs to be examined closely, and it probably requires improvement. The only physical factor indicated by the result is the partitioning of events by depth. This can also be viewed as an operational factor in that the scaling of discriminants by depth may improve the performance of the discriminants.

F. OPERATIONAL PROBLEMS

The purpose in clustering events using multiple discriminants is to characterize earthquakes and explosions by their 'like' discriminant patterns. In performing such analyses, several operational problems were identified; these include:

- A scaling problem with some of the discriminants, as was indicated by the dependence of clustering on event magnitude.
- A bias problem caused by network averaging, as was indicated by the dependence of clustering on the number of station detections for a given event (i.e., events with less than two network detections were clustered).
- A station bias and variance problem which was caused by the leakage of energy from outside of the spectral band of the filters which were used to measure the variable frequency magnitudes.

The magnitude scaling problem flagged by cluster analysis must be resolved. Otherwise, discrimination performance could

be misleading because of the dependence of the results on superfluous factors such as the magnitude of the earthquake and explosion populations. Using the Priority II network together with some other stations, the discriminants were scaled by setting each of the discriminants equal to a function of network magnitude, $F(m_b)$. In particular, linear scaling was performed, where $F(m_b) = c m_b + d$. The parameters c and d reflect the magnitude dependence of the discriminants. A robust method developed by Claerbout (1976) was used to determine the value of the parameters for each discriminant. Only those discriminants for which the variance was significantly reduced by the scaling process were scaled.

Figure II-2 showed the baseline discriminants which evidenced operational problems (in particular, magnitude-dependent clustering). Figure II-10 shows the results obtained by appropriate scaling of each discriminant to remove network magnitude dependence. Note that discriminants involving surface wave magnitudes required non-linear scaling, with the break-point in the linear trend at $m_b=4.9$. The trend curves for groups of larger and smaller magnitude events were obtained by scaling clusters of large and small groupings of shallow earthquakes. In general, the non-linear scaling of discriminants which are associated with surface wave measures significantly reduced the variance of the discriminant values; this was not the case for discriminants involving short-period P wave magnitudes. The results shown here for magnitude scaling were taken from Sax, et al. (1979).

FIGURE II-10
 SCALED DISCRIMINANTS $D_I = F(m_b)$

$D_1 = 3.5 [M_s - M_s(50) - 0.10]$	
$D_2 = 2.5 [0.55m_b + M_s(14) - M_s - 1.89]$	$m_b < 4.9$
$2.5 [m_b + M_s(14) - M_s - 4.10]$	$m_b \geq 4.9$
$D_3 = 1.0 [m_b(0.5) - m_b(0.3) - 0.3m_b + 1.84]$	
$D_4 = 1/3 [m_b(0.8) - m_b(0.5) - 0.33m_b + 2.17]$	
$D_5 = 2.5 [0.34m_b + M_s(14) - M_s(17) - 0.92]$	$m_b < 4.9$
$2.5 [0.54m_b + M_s(14) - M_s(17) - 1.90]$	$m_b \geq 4.9$
$D_6 = 2.5 [1.30m_b - M_s - 1.18]$	$m_b < 4.9$
$2.5 [1.71m_b - M_s - 3.19]$	$m_b \geq 4.9$
$D_7 = 2/3 [1.24m_b - M_s(50) - 0.97]$	$m_b < 4.9$
$2/3 [1.86m_b - M_s(50) - 4.01]$	$m_b \geq 4.9$
$D_8 = 3.0 [0.81m_b - m_b(0.3) + 1.14]$	
$D_9 = 2.5 [m_b(3.2) - m_b(0.3) + 3.96]$	
$D_{10} = 12 [F - \bar{\sigma}_\phi]$	
$D_{11} = 1/2 [m_b(1.3) - m_b(0.8) + 0.14m_b - 0.23]$	
$D_{12} = 1.5 [m_b(2.0) - m_b(0.5) + 1.67]$	
$D_{13} = 3.5 [{}_0\int^5 A^2 dt / {}_5\int^{10} A^2 dt - 0.35]$	
$D_{14} = 1.0 [1.67 D_{12} + D_6]$	
$D_{15} = 1.5 [3 D_{10} + 5 D_{11}]$	
$D_{16} = 2.0 [3 D_{10} + D_6]$	
$D_{17} = 2.5 [3 D_{10} + D_9]$	
$D_{18} = 1.5 [3 D_{10} + 1.67 D_{12}]$	

As a result of applying the scaled discriminants, the eight clusters obtained by training on earthquakes merged into a single earthquake cluster. This result indicates that the clustering of our baseline discriminants appeared to stem from the magnitude scaling problem. Further, we now know the importance of removing operational problems before gauging the effectiveness of the discriminants used.

SECTION III
EVENT IDENTIFICATION SYSTEM - METHOD

Our method of event identification involves six basic analysis procedures (see Figure III-1). Given the complicated nature of the identification problem, it is useful to review some of our general observations and concerns about the analysis procedures used; these are summarized in Table III-1. Detailed, amplifying material, is provided below.

A. ACCESS SIGNAL TIME WINDOWS

1. Short-period signals

Short-period signals are accessed at estimated arrival times computed from reported focal parameters. These parameters are origin time, location, and depth of the event. We found that errors in these parameters make it necessary to start the edit process by sampling four-minute records. An automatic detector then compresses these larger records to smaller one-minute, signal-centered edits. Next, signal measurements are performed and classified as signals or noise by an automatic decision process. These signal or noise measurements are then stored on standard format magnetic tape records. The automatic detector for accessing short-period data and initializing the measurement of seismic signals is described in Appendix A.

FIGURE III-1
EVENT IDENTIFICATION SYSTEM ANALYSIS PROCEDURES

- ACCESS SIGNAL TIME WINDOWS
- EXTRACT SIGNAL WAVEFORMS
- MEASURE SIGNALS OR NOISE
- ESTIMATE SOURCE PARAMETERS
- COMPUTE DISCRIMINANTS
- CLASSIFY EVENTS USING CLUSTER ANALYSIS
 - EARTHQUAKE CLUSTERS
 - EXPLOSION CLUSTERS

TABLE III-1
 EVENT IDENTIFICATION SYSTEM - SUMMARY
 (PAGE 1 OF 3)

Analysis Procedure	Description	Observations/Concerns/Problems	Amplifying Material Subsection	Page
ACCESS SIGNAL TIME WINDOWS	<p>Arrival times for short-period phases were computed from reported time, location, and depth of event. For objectivity, it was preferable to use an automatic detector. In the current study, Unger's (1978) automatic detector was used (detector operates on time sequences of instantaneous amplitude and phase measurements). The determination of long-period arrival times presented no problem.</p>	<p>Unger's detector produced a negligible number of false alarms. Almost all detected short-period signals were accurately timed. Where signals were not detected, they were either emergent or exhibited short, impulsive signatures. Automatic timing of arrivals from multiple events is a problem. The problem of short-period P-wave extraction would be significantly alleviated if more precise location and depth estimates are made available. The automatic detector was not needed for long-period signal detection.</p>	A	III-1
EXTRACT SIGNAL WAVEFORMS	<p>Extraction of strong signals presented no problem, and was done based on detections made using Unger's detector. The extraction of long-period signals was accomplished using time windows based on surface wave propagation times.</p>	<p>Advanced signal analysis techniques will be needed to extract waveforms of weak signals obscured by interfering noise. Such techniques include, but are not limited to, adaptive beamforming (ABF) and polarization filtering. In cases where no signals were detected, magnitude estimates were made using noise in the signal arrival window; this situation should be alleviated, and it does require further study.</p>	B	III-9

TABLE III-1
 EVENT IDENTIFICATION SYSTEM - SUMMARY
 (PAGE 2 OF 3)

Analysis Procedure	Description	Observations/Concerns/Problems	Amplifying Material Subsection Page
MEASURE SIGNALS OR NOISE	<p>Instrument response corrections made in order to obtain consistent measurements of ground motion. Further, data were bandpass filtered to obtain accurate frequency-dependent station magnitude measurements. Gaussian bandpass filters were used. Complexity was computed as the energy ratio of the acceleration waveform envelope integrated from 5 to 10 seconds after the signal start time, to that integrated from 0 to 5 seconds; 'pulse complexity' (Unger, 1978) was also computed.</p>	<p>Analog system response is not equivalent to the system response represented by sampled digitized data; this was accounted for in this study. With regard to bandpass filtering of data, the main design problem is to provide sufficient frequency resolution consistent with an adequate resolution of the envelope peaks of signals occurring in the signal time window. Spectral leakage was another problem encountered; the effect of such leakage was minimized through the use of a spectral amplitude threshold criterion. A procedure for minimizing spectral leakage, involving spectral whitening, is discussed.</p>	C III-10
ESTIMATE SOURCE PARAMETERS	<p>Source parameters are derived from signal measurements described above. Most of the source parameters used as a basis for discriminating between earthquakes and explosions are derived from the broadband and spectral magnitudes of propagated seismic phases. Ringdal's (1975) method, as modified in this study, is used for estimating unbiased source magnitudes by combining magnitudes of detected signals with magnitudes determined from noise.</p>	<p>Ringdal's (1975) method should be modified to handle more effectively the case of few detections; alternatively, only data for which detections are made at three stations should be used. There is considerable observational evidence that station magnitude bias should be carefully taken into account together with station noise when applying Ringdal's maximum likelihood technique to determine unbiased p-wave event magnitudes.</p>	D III-22

TABLE III-1
 EVENT IDENTIFICATION SYSTEM - SUMMARY
 (PAGE 3 OF 3)

Analysis Procedure	Description	Observations/Concerns/Problems	Amplifying Material Subsection	Page
<p>COMPUTE DISCRIMINANTS</p>	<p>The fundamental bases for categorizing event types is by differences in spectral shape and by time domain measurements of pulse and coda complexity. In all, 18 discriminants are computed and used in this study. The use of these discriminants is based on the physics of explosion and earthquake sources.</p>	<p>Some discriminants are more effective than others in identifying source types. Thus, additional studied should be directed at eliminating ineffective discriminants, and in optimizing the performance of the effective ones. Magnitude scaling problems and other scaling dependencies are a potential problem area.</p>	E	III-27
<p>CLASSIFY EVENTS USING CLUSTER ANALYSIS</p>	<p>Cluster analysis enables the seismologist to comb files of seismic measurements in search of consistent discriminant patterns by which to identify event types or to correlate the behavior of a discriminant with a pattern of known event types previously encountered. A systems approach to cluster analysis further optimizes the application of this dynamic identification technique by maximizing the time a scientist has for actual data interpretation.</p>	<p>For cluster analysis to be effective, one must 'train' the identification system on earthquake data. No assumptions should be made (nor are made) about the characteristics of explosions. Four events with 'like' clustering characteristics are required here to define a cluster (and, presumably, an event type).</p>	F	III-38

The function of the short-period edit detector is to extract short P-wave signals of several seconds duration from a much longer seismic record. The edit problem is complicated by non-stationary seismic noise, system noise, and interfering seismic signals. The diversity of seismic signals (emergent, impulsive, 'multipathed', coda scattered, etc.) causes problems in designing an effective automatic edit detector which operates well under all conditions. Thus, although the short-period automatic edit process now used performed well, it can be improved, and additional study of such edit processors is recommended.

2. Long-period signals

Analytical dispersion relationships are shown on Figure III-2. These relationships predict frequency-dependent arrival times of dispersed surface waves. The analytical relationship is used to automatically set the start and end time of a signal edit window which is to be processed by narrowband Gaussian filters. Magnitudes are computed by searching for the maximum amplitude in these frequency-dependent time windows. The edit's detection status as signal or noise is determined by a threshold set 12 dB above the mean noise level. This noise level is measured in a time window preceding the signal edit window. There was no need for a signal detector, as was the case for short-period signal editing, because the signal windows encountered are a large fraction of the window predicted by the analytical dispersion relationships.

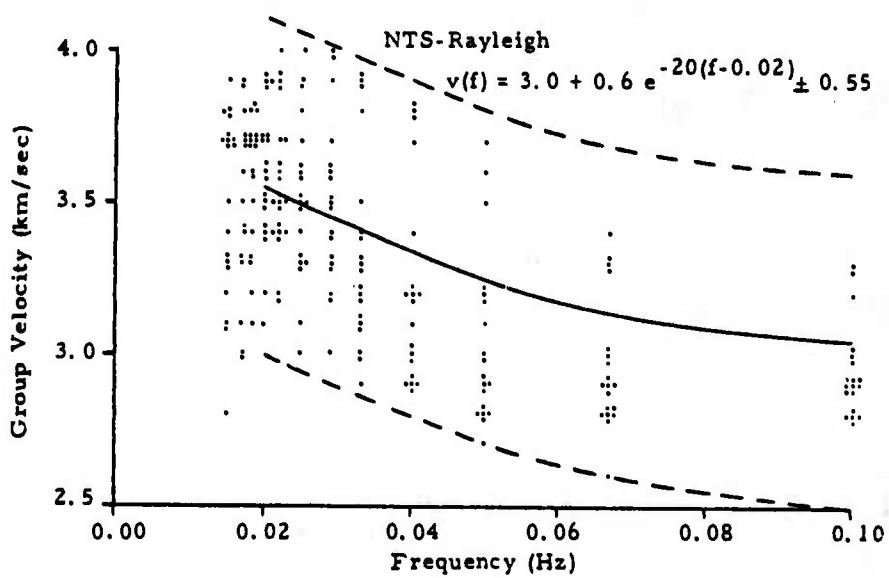
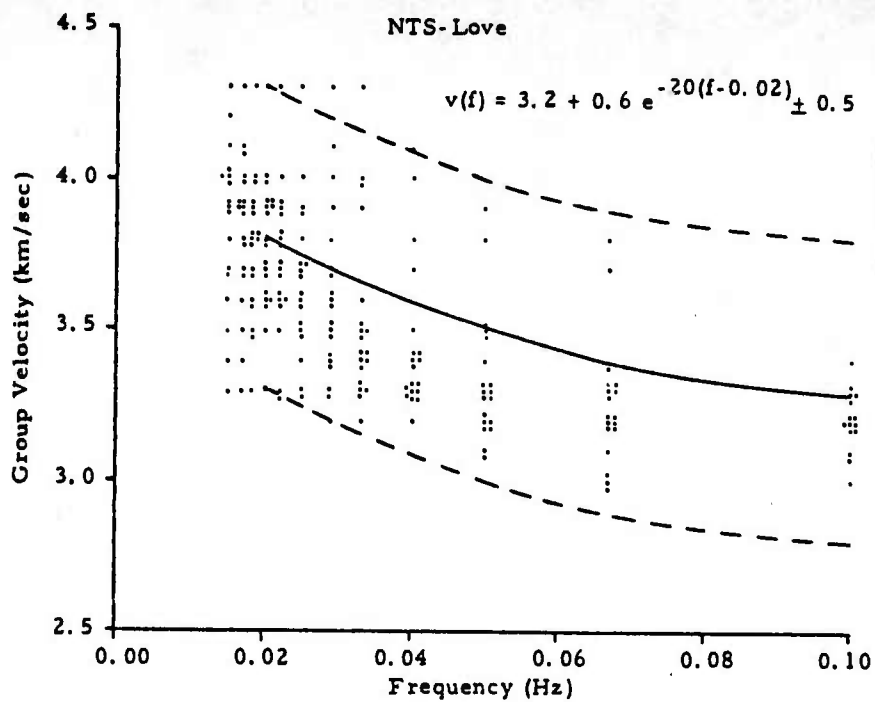


FIGURE III-2
DISPERSION FOR WORLD-WIDE STATIONS
(PAGE 1 OF 2)

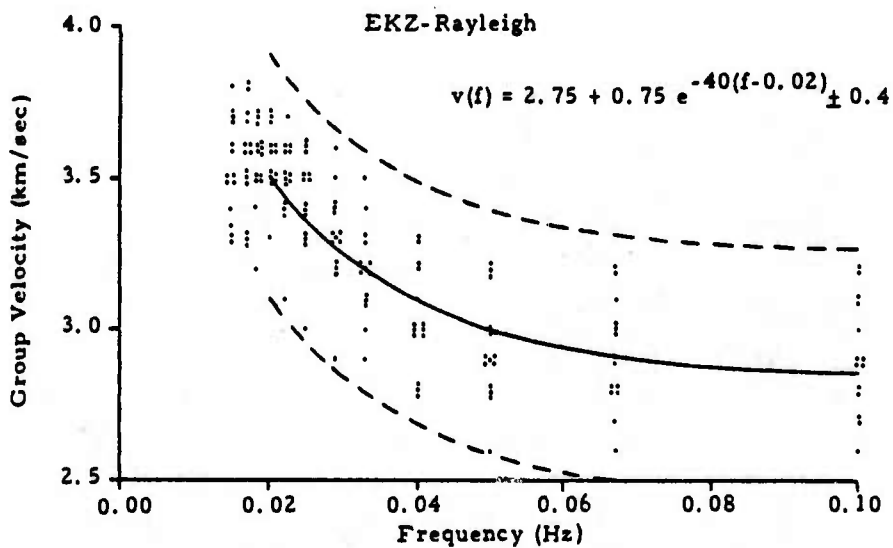
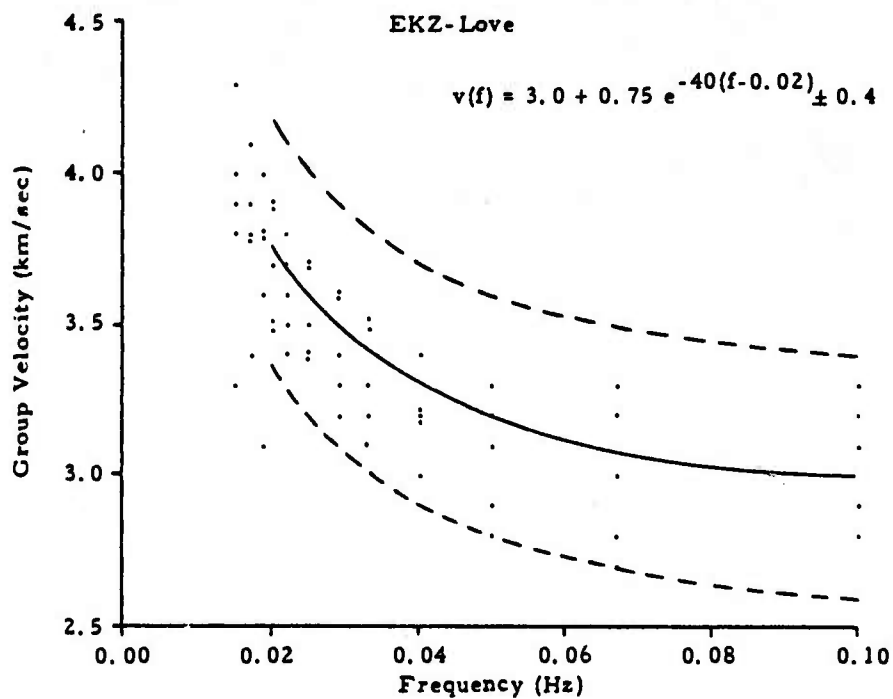


FIGURE III-2
DISPERSION FOR WORLD-WIDE STATIONS
(PAGE 2 OF 2)

B. EXTRACT SIGNAL WAVEFORMS

Extracting the waveform of a strong signal presents no problem, but advanced signal analysis techniques appear necessary to effectively extract weak signals which are obscured by interfering noise. Presently, we are editing signals without the benefit of such advanced techniques. Thus, half of our events had only one or no detected signals, and cluster analysis indicated that problems existed in interpreting these signals.

The following extraction techniques can be used to improve weak-signal detection and measurement:

- Beamforming and adaptive beamforming (ABF) of short-period and long-period array data.
- Polarization filtering of three-component, short-period records at regional distances.
- Polarization filtering of three-component, long-period phases.
- Fixed and adaptive Wiener filtering of single-sensor and three-component sensor data.
- Complex cepstral analysis (to reduce interferences between ambient and coda noise).

These signal analysis techniques should eventually be tested, calibrated, and integrated into the signal edit process.

C. MEASURE SIGNALS OR NOISE

In part, our baseline approach to earthquake and explosion identification depends on the availability of accurate frequency-dependent magnitude measurements of seismic signals. In many cases, smaller signals are invisible because of seismic noise. This leads to biased sampling of the larger signals in order to derive event magnitude measurements. To eliminate this bias, Ringdal (1974, 1975) developed a maximum likelihood technique for unbiased estimates of event magnitude. This technique modeled the deviations of signal magnitudes as normal statistics. This and other techniques of event parameterization will be considered later. First, however, we describe below the techniques used to obtain high quality measurements of the seismic signals which are used as input to an event source parameter measurement process.

1. Instrument response correction

Different seismic sensors used in the Priority II network exhibit significant variations in their frequency response to earth motion. Therefore, instrument response corrections are needed to obtain consistent measurements of ground motion. A simple analog approach to making instrument response corrections is to fit instrument calibration data by the ratio of rational polynomials of s , where $s=i\omega$. In particular, the polynomials represent the system response as

$$A(s) = \frac{\prod_j (s+a_j)}{\prod_j (s+a_k)} \quad \begin{array}{l} \text{zeros} \\ \text{poles.} \end{array}$$

Determination of $A(s)$ is obtained graphically by corner frequency analysis of log-log plots of the calibrated displacement amplitude versus frequency. Corner frequencies of zeros are indicated by frequencies above which the log-log slope increases by 6 dB/octave; poles, by -6 dB/octave. This procedure approximates analog response curves to within an accuracy of at least 10%. Note, in passing, that this model approximates the phase as well as the amplitude response of the system. Filters to invert the system response are readily implemented by inverting these zeros and poles. This time-domain approach removes the amplitude and phase response of the system at all frequencies.

A point often overlooked is that the analog system response $A(s)$ is not equivalent to the digital system response of uniformly time-sampled data. Conversion of the real roots of $A(s)$, $(s+a)$, to real roots of a point sampled delay operator $(a-bZ^{-1})$, where $Z=\exp^{-i\omega T}$ and T is time between samples, is accomplished by invoking a criteria for impulse response invariance. That is, the sampled delay operator, transformed back to the time domain, has an impulsive response which is a time-sampled equivalent of the continuous analog impulse time function. For example, a Laplace-transformed pole representing an analog exponential response is equivalent to a digitally sampled exponential response as follows:

$$\frac{1}{s+a} \rightarrow \exp(-at) \quad t \geq 0$$

$$\frac{1}{a-bZ^{-1}} \rightarrow b^n = \exp(-anT) \quad (n=0,1,\dots,\infty)$$

where

$$b = \exp(-aT).$$

Thus, $A(s)$ is transformed to the equivalent impulse invariant sampled delay operator function,

$$B(Z) = \frac{\prod_j (1 - \exp(-a_j T) Z^{-1})}{\prod_k (1 - \exp(-a_k T) Z^{-1})}$$

The effect of each pole is exactly removed by successively applying a difference operator,

$$y_i = x_i - b_k x_{i-1}, \quad \text{where} \quad b_k = \exp(-a_k T).$$

This operation is stable, presents no problem with roundoff errors, and tends to reduce the interference of signals with microseismic noise. Complex poles are similarly removed by second order difference operators; these, too, are stable.

Since the zero's of the system response occur at multiple roots near zero frequency, their removal is accomplished rigorously by numerical integration, $y_i = y_{i-1} + x_i$. Since the root modulus, $|Z| = 1$, is on the unit circle in the Z-plane, the operation is quasi-stable leading to errors at low frequency caused by amplification of seismic noise and drift errors due to integration of roundoff errors. Consequently, the inverse of a low frequency zero is performed approximately as

$$y_i = c_j y_{i-1} + x_i + d_{jm} \sum_{\ell} F_m(t_i - t_{\ell}) x(t_{\ell}),$$

where the recursively filtered component y_i is augmented by the weighted output of a bank of narrowband filters, F_m

(which approximate the system response at low frequencies). This operation is stable and accurate between 0.2 Hz and the Nyquist frequency. Selection of constants c_j , d_{jm} , and narrow bandpass filters are designed to invert the system response with a maximum error less than 20%, and to provide a stable inverse of the system response zeros.

2. Application of bandpass filters to measure frequency dependent magnitudes

One purpose of filtering seismic signals is to obtain accurate, frequency-dependent station magnitude measurements. Such measurements are our main source of data for characterizing seismic source mechanisms.

Physical validation of any derived relationship between station magnitude measurements and source mechanism depends on properly scaling amplitude measurements with distance and depth. It is expected that a number of different frequency-dependent magnitudes must be measured to uniquely describe and identify different rupture mechanisms (e.g., shear, tensile, and compressional dislocations). Environmental factors such as source depth, regional crustal geology, and tectonics, as well as such physical factors as stress, stress drop, and source dimension, are expected to influence the relationship between frequency-dependent magnitude and source mechanism. A summary of these factors expected to influence the physical validity of magnitude models is given in Figure III-3.

The design of optimized bandpass filters for variable frequency magnitude measurements is described in Appendix B.

FIGURE III-3
PHYSICAL VALIDITY OF MAGNITUDE MEASUREMENTS

- PROPER SCALING
 - DISTANCE-ATTENUATION
 - DEPTH

- COMPLETENESS
 - DIFFERENT RUPTURE MECHANISMS
 - DIFFERENT MEDIUM PROPERTIES

- PHYSICAL PARTITIONING
 - DEPTH OF SOURCE
 - STRESS, STRESS DROP, PHYSICAL DIMENSION OF SOURCE
 - CRUSTAL GEOLOGICAL AND TECTONIC ENVIRONMENT OF SOURCE AND RECEIVER.

This problem is of concern since filter-sideband-leakage errors can lead to significant magnitude bias errors and large variance of variable frequency magnitude measurements. These errors occur mainly at short periods above the corner frequency where the roll-off of the source spectrum and of absorption combine to cause the filtered signal to peak well outside of the filter passband (defined by the 3-dB-down points of the filter). Our experience indicates that the constraint of measuring magnitudes only at times when the dominant period of the signal is within the filter passband will only partially correct this problem (this was the technique used in the present study). Additional means are needed by which to perform band-limited magnitude measurement in those cases where the dominant period of the filtered signal is not within or is rarely within the prescribed frequency band limits.

3. A recommended procedure for eliminating spectral leakage errors from filtered magnitude measurements

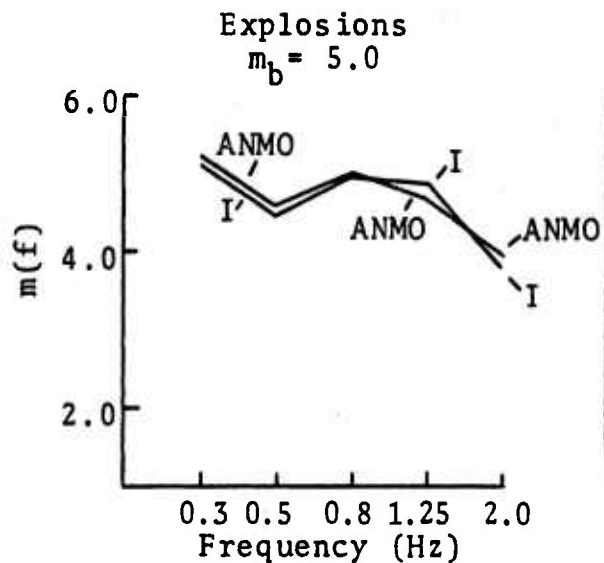
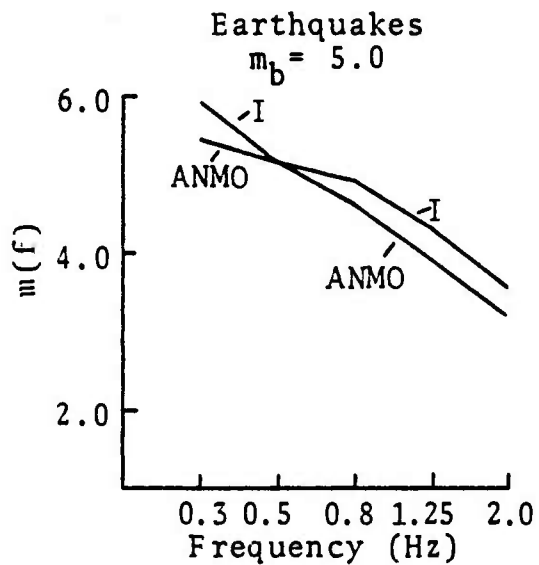
The following spectral whitening technique is a candidate procedure for reducing spectral leakage in future studies. First, remove the ground-displacement system response. Then, if the frequency corresponding to the measured magnitude (when the measurement is made at the dominant frequency) is below the specified filter passband, modify the ground motion measurements by successively applying a first difference operator, $y_i = x_i - x_{i-1}$, N times until this observed low frequency bias is removed. The amplitude spectrum is thus transformed by N stages of this difference operator; that is,

the spectrum is modified by the factor $|1 - \exp(-2\pi T f_p)|^N$, where T is the time between data samples and f_p is the dominant frequency of the measured displacement magnitude. Division by this factor, corrects the magnitude measurements for the effect of successive difference operators which were required to whiten the data in the passband of the filter.

The above technique should provide an efficient means by which to obtain high-resolution measurements of ground displacement magnitudes. Further, these measurements will be optimized for each filtered band. As such, the leakage problem associated with the filter bandwidth should be eliminated by application of this method.

A physical justification of this high-resolution technique is as follows. Above the corner frequency of a seismic signal, the spectrum is expected to roll-off as f^{-a} (where a is equal to one, two, or three). For $a=1$, envelope measurements of ground velocity are measured to compute magnitudes; for $a=2$, ground acceleration is measured; and for $a=3$, the first derivative of the ground acceleration is measured. Thus, the high resolution inverse operator $|1 - Z|^{-N}$ is specifically designed to whiten the spectrum for each filter band in accordance with the variable roll-off which characterizes the seismic source spectra. The results shown in Figure III-4 indicate that absorption alone does not appear to cause a leakage problem up to 2.0 Hz, but that absorption, combined with a spectral roll-off of f^{-a} , does cause a leakage problem. At higher frequencies, however, the increased roll-off due to absorption may require the use of a higher difference operator to whiten the spectra. These difference operations

ABSOLUTE MAGNITUDES



RELATIVE MAGNITUDES

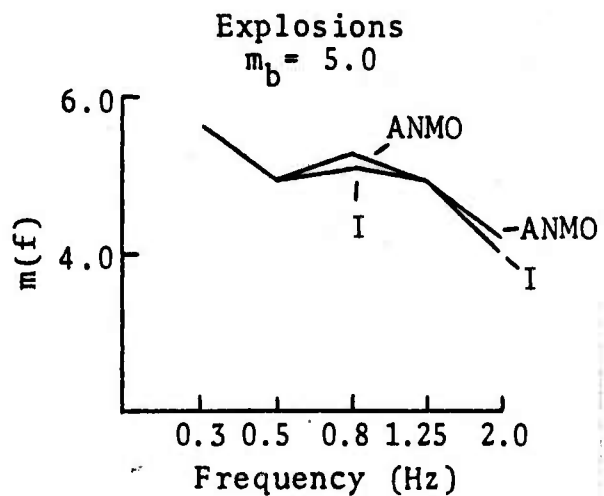
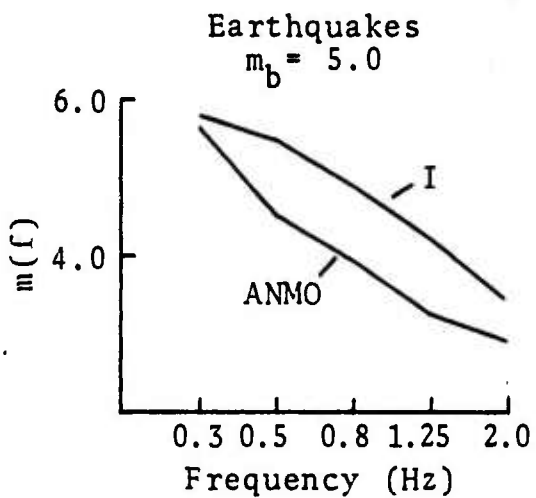


FIGURE III-4
COMPARISON OF FILTERED MAGNITUDE MEASUREMENTS
FOR STATIONS ANMO AND I

are stable and should, in general, enhance the signal-to-noise ratio in the band of the bandpass filter.

4. Time-domain measurements of complexity

An instrument response correction was applied to seismic waveforms to represent, as accurately as is possible, the ground displacement produced by seismic signals at each station. For purpose of measuring signal complexity, acceleration waveforms were generated by differentiating the displacement waveforms. The purpose in doing this and in selecting certain time windows was to accentuate scattering effects associated with a (presumed) complex earthquake source at frequencies above the corner frequency, and also, to reduce the effect of microseismic noise on the complexity measurement.

The coda complexity was computed as the energy ratio of the acceleration waveform envelope integrated from 5 to 10 seconds after the signal start time, to that integrated from 0 to 5 seconds. The first measure represents the energy in the signal while the second measure (from 5 to 10 seconds) gauges the coda characteristic. It was expected that pP effects from explosions would be contained in the onset window (0-5 seconds); pP effects from earthquakes, however, were expected to occur at times greater than 5 seconds after arrival onset. Even for deeper earthquakes, it is expected that heterogeneous crustal layers would not attenuate backscattered energy as rapidly as they would for shallow explosion sources. Thus, low values of this coda complexity are considered an indicator of shallow and less complex seismic sources. As a result, the complexity defined here should

gauge well the complexity characteristics of explosions and earthquakes. However, the use of the 5 and 10 second time windows in computing complexity are, to some extent, arbitrary. Clearly, the tradeoffs involved in making these coda complexity measurements need further study.

An even smaller-scale measure of complexity which was also used, referred to as 'pulse complexity,' was defined by Unger (1978). Using this method, the phase standard deviation and average frequency of the pulse are determined for the signal first motion from a model of phase versus elapsed time (measured from the onset of the signal). The derivation of these quantities are shown in Figure III-5.

Unger observed that for both earthquakes and explosions, a linear relationship exists between the dominant frequency of signals and their phase standard deviation. This is shown in Figure III-6. The linear trends of earthquakes and explosions (at least for the events examined) appear to be displaced enough to effectively separate the two populations. On the basis of the results discussed above, the pulse complexity discriminant was defined by Unger as the difference between the phase standard deviation and average pulse frequency. This discriminant measures the separation between the explosion and earthquake trend lines, and is based on the assumption that explosions are expected to be smaller and less complex sources than are earthquakes.

FIGURE III-5

DERIVATION OF PHASE STANDARD DEVIATION AND
AVERAGE FREQUENCY OF SHORT-PERIOD P WAVES

PULSE COMPLEXITY MEASUREMENTS

- Signal represented as modulated envelope and phase

$$x(\tau) = E(\tau) \cos\phi(\tau)$$

where $x(\tau)$ = the presumed signal waveform
 τ = elapsed time from the signal onset
 $\phi(\tau)$ = instantaneous phase measurement
 $E(\tau)$ = instantaneous envelope measurement
 T = length of signal time window.

- Least squares quadratic phase model; $\hat{\phi}$ fit to measured ϕ as

$$\hat{\phi}(\tau) = a_0 + a_1\tau + a_2\tau^2.$$

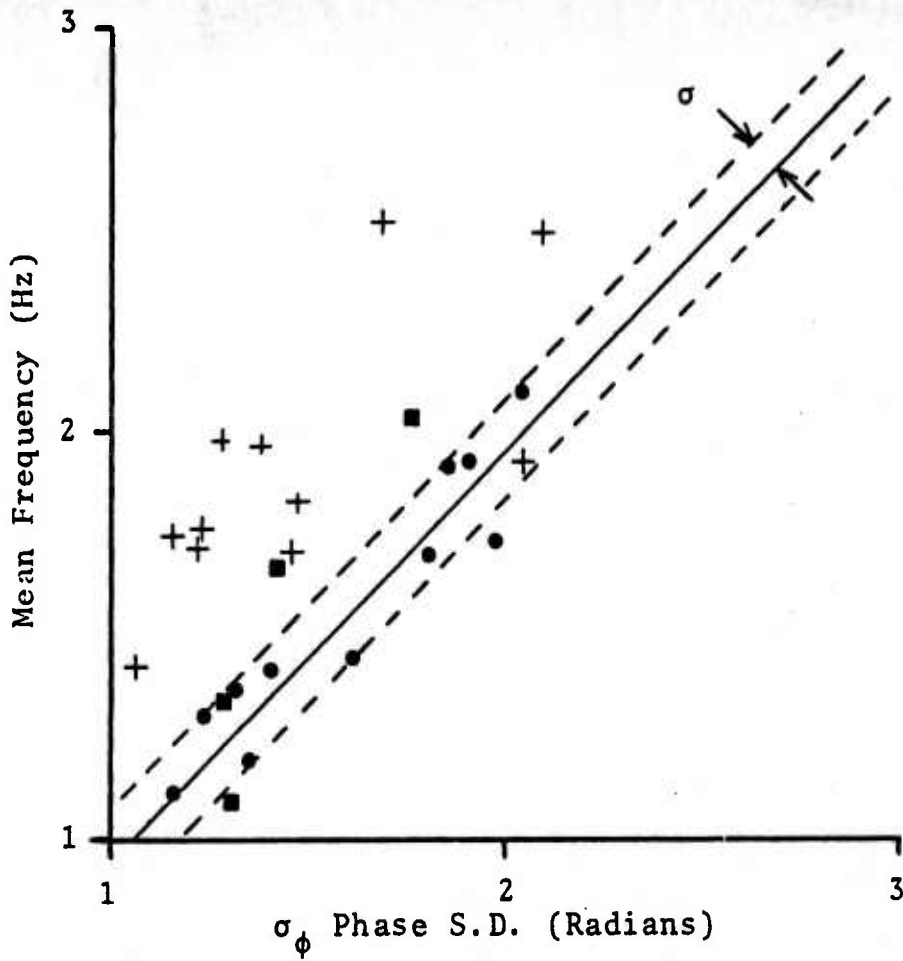
- Signal parameters
 - phase standard deviations

$$\sigma_{\phi} = \left\{ \frac{1}{T} \int_0^T [\phi(\tau) - \hat{\phi}(\tau)]^2 d\tau \right\}^{1/2}$$

- mean frequency

$$\bar{F} = \frac{1}{2\pi} [a_1 + T a_2].$$

- Pulse complexity: $\sigma_{\phi} - \bar{F}$.



- Normal shallow earthquake
- + Explosion event
- Unknown event
- σ One standard deviation

FIGURE III-6
 PULSE COMPLEXITY DISCRIMINANT $f-\sigma_{\phi}$

D. SOURCE PARAMETERS ESTIMATED FROM SIGNAL MEASUREMENTS

Source parameters are derived from the signal measurements described in the preceding section. One such parameter is the coda complexity of the source. To minimize the effect of multiple signal paths and later seismic phases, coda complexity is defined as the minimum value of station measurements of coda complexity. Only detected signals are used here. Other time-domain source parameters, which describe the dominant frequency and the phase variance of the initial acceleration of the source, are estimated by arithmetic averaging of signal measurements.

Most of the source parameters used as a basis for discriminating between earthquakes and explosions are derived from the broadband and spectral magnitudes of propagated seismic phases. These source parameters differentiate source types by means of the spectral 'shape' of the (perceived) emitted energy and by relative excitation of the propagated phases. There is some evidence that source magnitudes are biased by averaging only detected signals which exceed the noise. Ringdal (1975), however, developed a method for estimating unbiased source magnitudes by combining magnitudes of detected signals with noise magnitudes, the latter taken as upper-limit estimates of the source magnitude at non-detecting stations. Ringdal's method is to estimate unbiased source magnitudes by maximum likelihood fitting of a normal curve to magnitude deviations of signals propagated from the source. This procedure provides a basis for estimating jointly 1) the unbiased magnitude of the event, and 2) a normal model for variable absorption and path scattering of signals.

Strauss (1978) tested Ringdal's method on measurements of long-period surface waves recorded at ALPA. Significant positive bias was observed at probability of detections less than 0.9. Ringdal's method apparently removed this bias down to a station probability of detection of 0.25. Thus, the threshold for obtaining bias-free measurements of M_s was extended to smaller events (roughly 0.6 to 0.9 units lower in magnitude). At probability of detections less than 0.25, Ringdal's method was observed to overcorrect for bias; this suggests that underestimates of magnitudes will result for events having few detections. Our observations suggest that this problem is operationally significant in that cluster analysis segregated events with one or no detections. In order to examine Ringdal's method, and, possibly, to understand the observed problem of magnitude over-correction, we review Ringdal's method in Figure III-7. Here, too, we derive a modification of Ringdal's method which may more accurately determine magnitude when only a few detections are possible. The modification shown in Figure III-7 takes into account the conditional dependence of detected signals exceeding noise. The adequacy of this modification needs to be tested.

A simple example can be used to demonstrate the significance of equation (2) in Figure III-7. Assume 20 observations of noise and one observation of signal, all characterized by an equivalent magnitude, m . The maximum likelihood magnitude determined using Ringdal's method is, approximately, $(m-1.8\sigma)$; using the modified method, however, the magnitude is given as $(m-1.4\sigma)$. With large standard deviations of the signal population, σ , then this example illustrates that Ringdal's method yields a significant over-correction of the magnitude.

FIGURE III-7
 MAXIMUM LIKELIHOOD ESTIMATION OF
 UNBIASED EVENT MAGNITUDE

- Ringdal's method finds the mean magnitude μ and standard deviation σ which maximizes the probability of the observed network detection

$$P_{NET} = \prod_i p\left(\frac{m_i - \mu}{\sigma}\right) * \prod_j P\left(\frac{a_j - \mu}{\sigma}\right) \quad (1)$$

all detections all non-detections

where m_i are observed signal magnitudes
 a_j are observed noise magnitudes
 p probability density of signals
 P probability that signal is less than noise.

- Modification of Ringdal's method

$$P_{NET} = \prod_i \left[1 - P\left(\frac{b_i - \mu}{\sigma}\right) \right] p\left(\frac{m_i - \mu}{\sigma}\right) * \prod_j P\left(\frac{a_j - \mu}{\sigma}\right) \quad (2)$$

where b_i is the observed noise magnitude associated with a signal magnitude m_i .

- Logical statement of the modified network probability
 - at detection stations, the signal exceeds noise and is detected
 - at non-detecting stations the signal is less than observed noise.

It is suggested that Ringdal's method either be modified and tested to handle more effectively the case of few detections or that thresholds be lowered sufficiently to insure that at least three stations detect an event. The latter strategy could be implemented by progressively lowering the threshold until signals are detected at stations where the expected noise magnitude is less than the network-determined event magnitude (i.e., at stations where the probability of detection is at least 50%). This provides a tradeoff of noise effects for, perhaps, larger errors in the magnitude estimates.

Network determinations of short-period P-wave magnitudes present other problems. Upper-mantle absorption and crustal scattering can affect both signals and noise in the same way. For example, upper mantle absorption can reduce the magnitude of trapped mantle modes made up of noise, as well as it can attenuate a P-wave signal. Observational evidence for this was cited by Dietz and Sax (1978), who used seismic station magnitude-bias observations prepared by North (1977) and by Evernden and Kohler (1976). Then, too, seismic noise observations of Fix, et al. (1973), Evernden and Kohler (1976), Hair, et al. (1964), and others, were also analyzed for this effect. These results have implications relative to the validity of Ringdal's method for computing unbiased P-wave magnitudes as follows.

Ringdal's method assumes a model in which noise levels and magnitude deviations are statistically independent. On the other hand, Dietz and Sax observed several noise groups for which a strong linear relationship existed between noise

levels and magnitude deviations. These apparent noise groups were considered to be significant because they had noise magnitude standard deviations of less than 0.1 units. Four such groups were observed with mean zero-to-peak noise levels of 1.6, 3.8, 9.1, and 15.8 μm which extended geographically over large regions. These are interpreted by us as being primarily composed of mantle noise modes at the quietest sites, of trapped crustal and sedimentary structure-related Rayleigh wave modes at still noisier sites, and of propagating ocean-generated noise at the noisiest stations (these were situated near coastlines). Stations within each group exhibited a large correlation of seismic noise with magnitude bias (e.g., higher noise levels appear to be associated with positive magnitude deviations). Thus, there is some observational evidence that station magnitude bias should be carefully taken into account, together with the station noise, when applying the maximum likelihood technique to determine unbiased P-wave event magnitudes.

Some problems were also encountered in combining magnitude measurements at various stations to determine the event magnitude. Some stations are observed to be more effective in discriminating event types. This suggests the possibility of degrading seriously the event discrimination capability of a network by averaging data for stations having good discrimination capabilities with those which have poor capabilities. As discussed in subsection C above, this problem may stem, to some extent, from recognized problems associated with signal measurement techniques. Also, the maximum likelihood or other signal averaging techniques employed need to be carefully reexamined. Finally, path absorption and scattering

effects should possibly be more adequately accounted for in determining accurate event magnitudes. These areas of concern are left as subjects for future study.

To optimize the estimation of unbiased P-wave magnitudes, it is desirable to include station corrections in order to remove signal magnitude measurement bias. These corrections should also be applied to the noise magnitude measurements in order to remove any station selection bias. Our experience with cluster analysis indicates that spectral magnitude measurements of events with few detections presents a serious operational problem.

In sum, the present technique of estimating unbiased magnitudes needs to be carefully reexamined and modified.

E. COMPUTATION OF DISCRIMINANTS

Our baseline approach is to select plausible discriminants which reflect the physical differences between earthquakes and explosions. These selected discriminants are applied empirically to separate explosion and earthquake populations. Our approach is evolutionary in that ineffective discriminants will be dropped, and effective discriminants will be modified to optimize performance. In this work, all candidate discriminants were used.

1. Empirical basis of our methodology

Our strategy is to select what we believe to be a complete set of discriminants and to infer seismic source types by clustering; in performing this analysis we do not require that characteristics of the various source types be specified in advance. Instead, intensive training is to be performed on earthquake data. If available, this training could also be performed on synthetic data. The purpose of such training is to obtain tightly clustered distributions of the discriminants, and to relate observed discriminant patterns to known event types. Such training with earthquakes is considered essential before any attempt is made to identify explosions.

Initially, a set of discriminants was selected in order to categorize events by observable differences of spectral shape, and by time-domain measurements of pulse and coda complexity. To be acceptable, these discriminants are expected to provide a rational basis for separating explosions from earthquakes. Some discriminants are expected to be more effective in identifying earthquakes; others, more effective in identifying explosions. Regardless, the use of a large, diverse set of discriminants is expected to result in stable identification of seismic sources by providing sufficient information and sufficient redundancy of information to separate different source types by consistently observed discriminant patterns. Figure III-8 illustrates the physical basis and redundancy of the initially selected set of baseline discriminants. Subsection II-B gave a more detailed discussion of these baseline discriminants.

FIGURE III-8
PHYSICAL BASIS FOR DISCRIMINANTS

- SHORTER PERIOD SURFACE WAVES AND RISE IN LOW FREQUENCY P-WAVE SPECTRUM DUE TO SHALLOW DEPTH

$D_1 = M_s - M_s(50)$	$D_3 = m_b(0.5) - m_b(0.3)$
$D_2 = M_s(14) - M_s$	$D_4 = m_b(0.8) - m_b(0.5)$
$D_5 = M_s(14) - M_s(17)$	$D_{10} = \bar{F} - \bar{\sigma}_\phi$
- MORE EFFICIENT PRODUCTION OF P-WAVES AND LESS EFFICIENT PRODUCTION OF SHEAR WAVES

$D_6 = m_b - M_s$	$D_8 = m_b - m_b(0.3)$
$D_7 = m_b - M_s(50)$	
- SMALL, HIGH-STRESS AND FULL STRESS-DROP SOURCES

$D_{12} = m_b(2.0) - m_b(0.5)$	$D_{10} = \bar{F} - \bar{\sigma}_\phi$
$D_9 = m_b(3.0) - m_b(0.3)$	
- ELASTIC REBOUND OF SOURCE LEADING TO OVERSHOOT OF THE DISPLACEMENT PULSE AND TO ROLL-UP OF THE HIGH FREQUENCY SPECTRUM

$D_4 = m_b(0.8) - m_b(0.5)$	$D_{12} = m_b(2.0) - m_b(0.5)$
$D_{11} = m_b(1.3) - m_b(0.8)$	$D_9 = m_b(3.0) - m_b(0.3)$
- LESS BACKSCATTER FROM SMALLER, SHALLOW SOURCE OR LESS COMPLEX SOURCE

$D_{13} = \text{Coda Complexity}$
 $D_{10} = \text{Pulse Complexity } \bar{F} - \bar{\sigma}_\phi$
- COMBINED EFFECTS

$D_{14} = D_{12} + D_6$	$D_{17} = 3D_{10} + D_9$
$D_{15} = 3D_{10} + D_{11}$	$D_{18} = 3D_{10} + D_{12}$
$D_{16} = 3D_{10} + D_6$	

Sometimes, discriminant clusters will exhibit operational problems. Events, for example, separate because of their limited range in magnitude, epicentral distance, focal depth, source/station tectonic classification, number of detected signals, etc. It should be possible to correct such operational problems by proper magnitude scaling of the discriminants, and by inclusion of adequate spectral corrections and of corrections for distance.

Magnitude scaling problems and other scaling dependencies are expected for a fixed set of spectral discriminants. For example, larger events are expected to have lower corner frequencies than those observed for smaller events. Consider two approaches to handle this particular scaling problem. One approach is to abandon fixed filters and to scale the center frequency of the bandpass filters to a fixed ratio of the corner frequency. However, since these corner frequencies are not easily measured, we took another approach. Specifically, we computed magnitudes using fixed spectral bands. On that basis, discriminants based on spectral shape eventually had to be subjected to m_b scaling (as is outlined in Figure III-9). Other signal or event measurement scaling problems involving source-to-receiver distance, absorption, depth, etc., can be treated in a similar way. Cluster analysis can provide an efficient means of detecting these dependencies.

2. Physical basis of discrimination

To be reviewed are some of the expected spectral and time-domain characteristics of earthquakes and explosions. Specifically discussed are differences in these characteristics for earthquakes and explosions, and in particular, the

FIGURE III-9
PROCEDURE FOR m_b SCALING OF DISCRIMINANTS

DISCRIMINANT SCALING METHODOLOGY

- Small and large normal shallow earthquake discriminant models are grouped by cluster analysis.

- Initial model for i^{th} and j^{th} frequency band

$$D_{ij} = m(f_i) - m(f_j) = c = \text{constant.}$$

- Determine the linear scaling model which minimizes the variance

$$D_{ij} = m(f_i) - m(f_j) = a + b m_b$$

where a and b are scaling constants and m_b is the network magnitude of the event.

- Possible non-linear scaling is determined by determining a and b separately for the large and small earthquakes.

rationale for using spectral shape and complexity as primary criteria for differentiating event types.

a. Physics of earthquake sources

A basis for discrimination is the expected spectrum of earthquakes in terms of a rupture growth model described by Archambeau (1979, personal communication). To first order, such sources are characterized by a quadrupole component. The low frequency spectrum scales as a source volume proportional to the final dimension of the rupture. At higher frequencies, a quadrupole corner frequency is inversely proportional to the compressional velocity (according to a two-thirds power law) and to rupture velocity (according to a one-third power law). For very low rupture velocities, the corner frequency is lower, and the roll-off of amplitude with frequency varies as f^{-1} to f^{-2} over a considerable frequency range before rolling off as f^{-3} . For rupture rates approaching the shear velocity, the f^{-3} roll-off occurs abruptly above the quadrupole corner frequency. Shock-driven rupture rates which greatly exceed the shear velocity are not expected; if encountered, however, they result in f^{-2} roll-off above the corner frequency. The quadrupole spectrum of shear waves is similar to that for P waves except that the former have a flat low-frequency component which is about five times that of P waves. The corner frequency of shear waves is expected to be slightly lower than that for P waves (about two-thirds that of compressional waves).

Higher-order multipole components emitted from earthquake sources are due to variations in initial stress,

material properties, and rupture velocity. These components are generated on a time scale less than that associated with the quadrupole corner frequency. The effect, which is highly directional, tends to mask the quadrupole corner frequency. It also distorts the signal by producing apparently large high-frequency peaks or holes in the spectrum due to constructive or destructive interference of multiple arrivals from multipole components. It can be argued hypothetically that the first arriving time terms of the signal are representative of homogeneous prestress conditions which existed at the time of the initial rupture. These are followed by higher multipole components which are caused by source complexity, and which propagate as multiple pulses having different group arrival times. These multiple pulses will have time-of-arrival separations which are dependent on spatial separations of stress concentrations, and on spatial variations of material properties within the rupture envelope. The effects produced by these higher multipole components have a strong azimuthal dependence, and exhibit large variations in dominant period, station magnitude, and frequency band magnitude. Because of contributions from multiple components, observational corner frequencies can be expected to shift to higher frequencies by as much as an octave. Yet, at some azimuths, the source may appear homogeneous by its exhibiting the expected quadrupole spectrum, unencumbered by source complexity effects. These source factors are further complicated by path and receiver absorption, and by scattering effects. These effects point out the difficulty of reducing magnitude measurements to event related parameters. If not taken into account by regionalization models, higher-order multipole moments can cause severe variance problems in any selected set of discriminants.

b. Physics of nuclear explosion sources, and a comparison of earthquake and explosion characteristics

Initially, vaporization produces a cavity of radius R_c . The material beyond R_c is liquified by a strong shock front to radius R_f . Beyond R_f , the material is subjected to pore collapse and plastic flow to radius R_p . Beyond the plastic radius, R_p , macrocracks and partial pore collapse occurs to the elastic radius, R_o . The detailed behavior of rock material as a result of this sequence of actions depends on equations of state for the material involved. Order-of-magnitude variations in some material parameters, especially those for near-surface crustal rocks, can result in significant variations in the spectrum of compressional waves which are produced by the explosion process. The most important variables influencing the character of seismic signals are the strength and void porosity of the material. Despite the diversity of signals produced by nuclear explosion sources, however, certain common features have been observed.

A common feature of explosion signals is the enhanced emission of compressional waves in all directions (as compared to earthquake signals). For an ideal, purely compressional monopole component emitted from the explosion cavity, the displacement spectrum increases linearly with frequency. This contrasts with the flat, low-frequency quadrupole term which is a dominant component of earthquake signals. This explosion-related effect, together with the destructive interference which results from the free surface reflection, should make it difficult, at long periods (~20 seconds), to

see waves emitted directly from a cavity which is buried at depths of about one-half kilometer. That such waves are clearly visible for explosions, however, indicates that a significant secondary mechanism for generating long-period surface wave signals exists. Tectonic release associated with explosions provides such a mechanism.

Some recent results of Rivers (1979) and Hsiao (1978) indicate, from analysis of long-period surface waves, that tectonic prestress is released at depths of several kilometers below an explosion cavity. This seems plausible in that higher rigidities and higher concentrations of prestress may be encountered at deeper depths. Further, it was observed that the tectonic release mechanism, as observed using long-period signals, is almost purely deviatoric, indicating a purely shear type source. These results suggest that the long-period waves are 'seeing' a secondary tectonic release mechanism in rigid crustal strata underlying the source, and for the most part, they are 'not seeing' the energy emitted uniformly at the cavity boundary.

The material above is interpreted as follows. At short-periods (~1 second), one expects to see a predominant monopole component of compressional waves which is uniformly emitted from the explosion cavity. This component is expected to be combined with a smaller quadrupole component which represents tectonic release. At long-periods (~20 seconds), only the quadrupole tectonic release part of the source is apparently seen. At long-periods, too, the monopole component of cavity emission is invisible as a result of the linear

decrease with frequency of the monopole component, and, in part, as a result of destructive interference produced by the free surface reflection.

Another significant secondary mechanism can affect the spectrum of some explosions. Shallow-focus explosions have been observed to exhibit strong free surface interaction which is produced by the large tensile stresses associated with wave reflection at the free surface. This effect may be intense enough to split rocks at their bedding planes and along pre-existing fractures. In such cases, the material can spall under large, normally oriented tensional tractions, and subsequently, will collapse because of gravity. This collapse process would result in a more complex signal at later lag times. In addition, high frequency scattering is expected as a result of opening and enlarging tensile fractures. This spall effect is expected to attenuate the surface-reflected depth phase, and to act as a low pass filter on the depth phase. This effect, then, further complicates explosion spectra.

Many explosions (and some earthquakes) exhibit time domain overshoot. This effect is characterized by a large-displacement spectrum peak just below the corner frequency. The physical mechanism responsible for overshoot is not well understood, but the effect on explosion signals is observed to be very material dependent. The effect can be interpreted as a medium-dependent impedance function applied to energy which is incident to the elastic boundary of the explosion. As such, the spectral signature called 'overshoot' may be useful to identify explosions by the excitation of high frequency P-wave magnitudes.

Factors influencing complexity also reflect differences between earthquake and explosion sources. Low stress drop events are probably associated with heterogeneously-distributed material properties within the rupture zone. Such complex events may yield variable time-lagged, higher-multiple components with spectral peaks at frequencies above the quadrupole corner frequency. This effect influences the pulse complexity measurement of ground acceleration seismograms. Signals of low stress drop events are also expected to contain higher dominant frequencies which are also observed to be associated with larger instantaneous frequency fluctuations. This observation of both earthquakes and explosions is the basis of our pulse complexity discriminant. The relationship for earthquakes and explosions is illustrated in Figure III-6. In general, signals from explosion sources of a given m_b tend to contain higher frequency components because the source is smaller than an equivalent earthquake. Explosive signals also tend to be lower in phase standard deviation because explosions are less complex sources. These relationships separate the populations, with the explosion populations interpreted as smaller, higher stress drop events than earthquakes.

c. Justification of the multiple discriminant approach

Observations of spectral shape and complexity over the full frequency range of measurements is the basis of our discrimination approach. It is justified by the many physical factors which influence seismic waves from earthquakes and explosions. This approach should result in a more

effective separation of the various possible types of earthquakes and explosions. We recognize that some discriminants are more powerful than others in separating certain types of events. Thus, care must be (and is) taken to avoid influencing the identification process adversely by unduly weighting weak discriminants. On the other hand, relying on only one or two discriminants increases the risk that the discrimination process will not separate all of the earthquake and explosion types which one is likely to encounter.

F. CLASSIFY EVENT TYPES BY CLUSTER ANALYSIS

The intent of any system used for event identification is to classify events as earthquakes or explosions. To this end, cluster analysis enables one to comb files of seismic measurements in search of consistent discriminant patterns by which to adaptively identify new event types or to associate an observed discriminant pattern with a known event population. In short, cluster analysis uses an efficient learning process to systematically classify events as earthquakes or explosions.

1. Systems approach to event identification

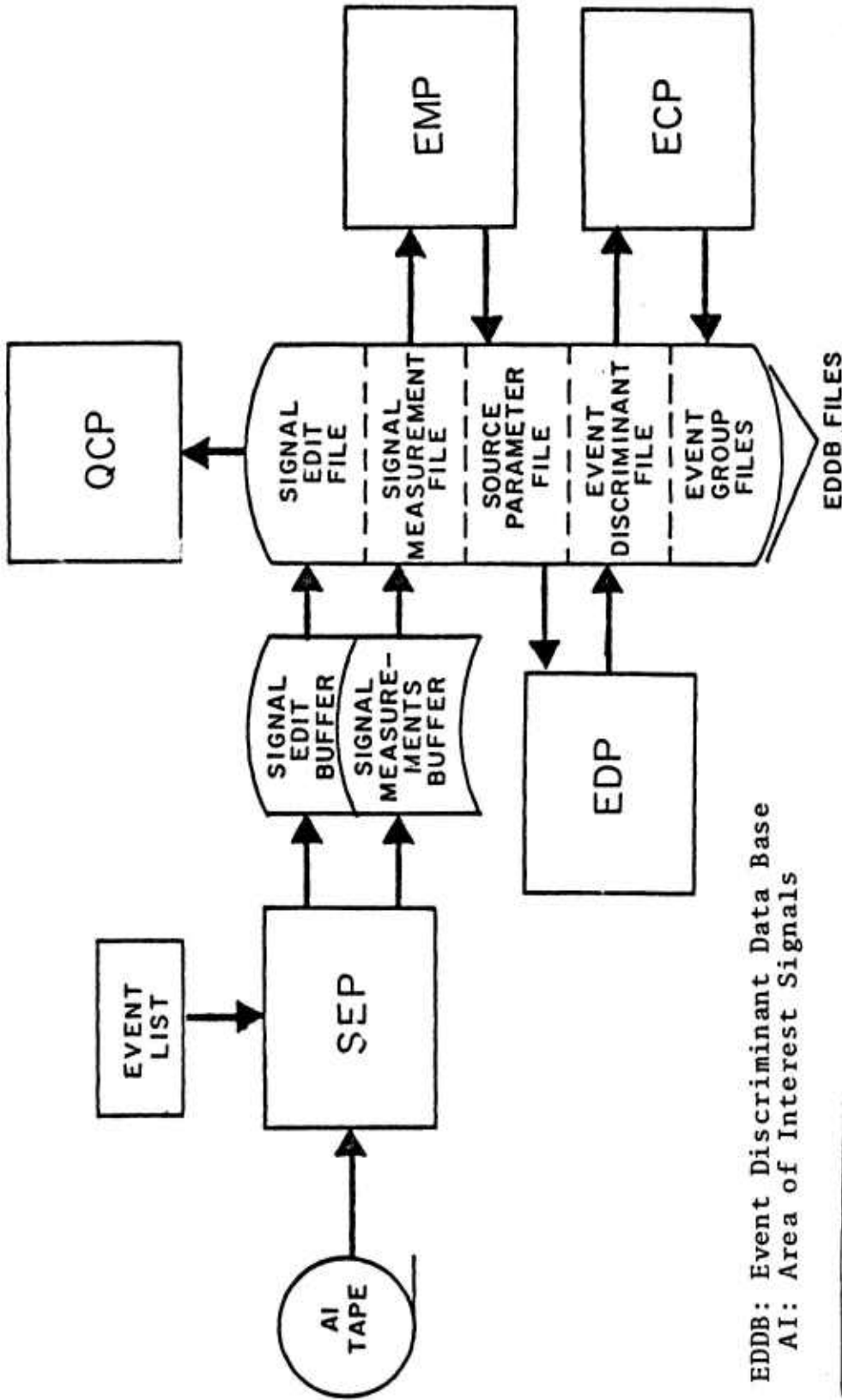
A highly automated adaptive system was developed to analyze edited signal waveforms, to estimate parameters characterizing propagated signals, to estimate source parameters from signal and noise measurements, and to classify events as earthquakes or explosions. The system maximizes the amount of time a scientist has for actual data interpretation.

It is linearly programmed to provide 'assembly line' processing. That is, the output of one processing function is taken as input to the next function, until classification of an event as an earthquake or an explosion is made. As shown in Figure III-10, each function sequentially generates files required by the event identification process. The functions are defined as follows:

- SEP - Signal Extraction Process inputs event locations and raw records of signals, it times the signal, measures parameters, and forms compressed edits of signal waveforms for further study, if needed.
- QCP - Quality Control Process provides for visual inspection of data.
- EMP - Event Measurement Process transforms measurements of signal parameters to measurements of event parameters; these parameters physically characterize the source.
- EDP - Event Discrimination Process generates a scratch file of discriminants to identify the event as an earthquake or an explosion.
- ECP - Event Classification Process identifies the event as an earthquake or an explosion based on 'cluster' analysis of the discriminants.

Permanent files are generated by the SEP to collect signal measurements which expand as the network adds more seismic stations. Also, this library of event information increases, as more 'users' are added to the system.

EVENT IDENTIFICATION SYSTEM
FUNCTION PROCESSES AND DATA FILE TRANSFORMATIONS



EDDB: Event Discriminant Data Base
AI: Area of Interest Signals

FIGURE III-10
SYSTEMATIC APPROACH TO EVENT DISCRIMINATION

2. Events with unknown discriminant patterns

The process of classifying events using discriminants is adaptive in that no prior knowledge of explosion discriminant patterns is required. Instead, after training on earthquakes (or even on synthetic data), any consistently observed discriminant clustering which cannot be associated with previously detected earthquake patterns is assumed to represent a new event type (possibly indicative of explosions). This adaptive discrimination algorithm is performed as follows (see, also, Figure III-11). Each discriminant component of the vectors is presumed to have been normalized such that normal earthquakes can be approximated as unit normal statistics; this was shown in Figure I-1. Events which exhibit abnormal discriminant patterns are interpreted initially as outliers of known normal earthquake populations. These events may (or may not) exhibit discriminant patterns which correlate better with the discriminant pattern of some other type of event. The problem of establishing such a new (anomalous) event type is to find several outliers with nearly identical discriminant patterns. These events are then classified as anomalous events or possible explosions. From physical considerations and experience, we expect to see several distinct types of earthquakes. It is therefore necessary to first train extensively on earthquakes so as to establish the patterns needed to identify these obvious earthquake types. As an initial step, these obvious earthquakes are associated with a known earthquake cluster and are removed from the data base of unknown events. The adaptive cluster analysis procedure is then used to identify the remaining events. Some of these events will ultimately be classified as possible explosions.

FIGURE III-11

INDUCTIVE PROCEDURE FOR DETECTING ANOMALOUS EVENT
GROUPS DISPLAYING CONSISTENT BUT UNKNOWN
DISCRIMINANT CHARACTERISTICS

ADAPTIVE DISCRIMINATION ALGORITHM

- Select a candidate outlier set i containing discriminant patterns D_i different from the normal event pattern D_N

$$|D_i - D_N| > \tau_1.$$

- Search set i for a pair of events $D_{A,1}$ and $D_{A,2}$ with the largest correlation product above threshold τ_2

$$[D_{A,1}, D_{A,2}] = \max\{D_m D_n\} > \tau_2 \quad m \neq n.$$

- Initialize the average anomalous discriminant pattern

$$\bar{D}_{A,2} = (D_{A,1} + D_{A,2})/2.$$

- Find other correlated events in set i and update the average anomalous discriminant pattern

$$D_{A,\ell} = \max\{D_m \bar{D}_{A,\ell-1}\} > \tau_2$$

$$\bar{D}_{A,\ell} = \frac{\ell-1}{\ell} \bar{D}_{A,\ell-1} + \frac{1}{\ell} D_{A,\ell} \quad (\ell \geq 3).$$

Decisions for clustering a group of events with a fixed, but unknown, discriminant pattern are controlled by three thresholds. The first decision is controlled by a threshold which is used to extract from the data base those events with a significantly different discriminant pattern. If a pair of these outlier events exhibits a high enough correlation product, their discriminants are averaged to initialize the (possibly new) anomalous event group. Other events with characteristics similar to those of this anomalous pair are sequentially associated to update the new discriminant pattern by averaging the discriminants. This association step is controlled by a second threshold which sets the criteria for determining whether the correlation product is high enough to indicate an acceptable degree of similarity between discriminant patterns. Finally, a third threshold is used to simply count the number of events in a cluster in order to determine whether to accept the group as a new event type. Presently, this last threshold is set to a count of at least four events. That is, the minimum number of events required here to establish the statistical parameters needed to characterize a new event group (following the procedure shown in Figure I-1).

An essential step of the adaptive clustering process is the calculation of correlation products between vectors which describe the observed discriminant patterns (referenced in Figure III-11). It is desirable to use large sets of discriminants in order to provide sufficient information and redundancy to separate reliably the different seismic source types. On the other hand, if too many weak discriminants are used, a noise problem is created in the computation of

the correlation products by mixing strong, effective discriminants with weak, (noisy) ineffective discriminants. We effectively resolved this problem by applying a non-linear algorithm to compute the correlation products. Normally a correlation product would simply be the dot product of two vectors, where each element of the vector is a discriminant normalized as is shown in Figure I-1. Here, however, each elemental product which is summed to obtain the dot product of two discriminant patterns is weighted by a zero or a one, depending on the following conditions. The weight is one:

- If each discriminant of the pair is above a prescribed threshold (in this study we used one as a threshold), and
- If each discriminant of the pair is of the same sign.

Otherwise, the weight is zero.

Computation of this threshold-controlled dot product effectively eliminates the accumulation of errors caused by the use of a large number of weak discriminants. In fact, if two uncorrelated discriminant patterns are modeled by unit normal statistics, the expected value of the correlation product is less than one (for eighteen discriminants applied with a threshold of one). In effect, this procedure reduces the accumulation of errors of eighteen discriminant elements to what would be expected from only a few discriminants. In cases where it is desirable to use even much larger discriminant sets (e.g., sets consisting of forty or fifty discriminants), this method could effectively control the errors accumulated in the clustering process by setting an even higher threshold criteria (e.g., a threshold of two).

Application of the above procedure does not require any a priori knowledge of the effectiveness of any particular discriminant, and it significantly improved the results we obtained with our set of baseline discriminants.

3. Event association by means of discriminant patterns

Events are identified as earthquakes or explosions by iterative application of adaptive cluster analysis. That is, cluster analysis is used to associate events with discriminant patterns (i.e., event types) previously established by cluster analysis.

The process is initialized by training on a large set of known earthquakes. The entire data base of earthquakes is set up as a normal reference group, and population statistics are determined. Cluster analysis of outliers is iteratively performed until the earthquake data base is decomposed into a number of clustered earthquake types having uniquely similar discriminant characteristics. Not all of the earthquakes will exhibit a similar enough discriminant pattern to associate with one of the clusters. These and explosion type events are expected to be dissimilar to the previously established earthquake clusters, and so, they should be rejected as members of any of the clusters.

Initialization is followed by an association process which is applied to the entire data base, including presumed explosions. The association procedure is shown in Figure III-12. This process extracts events which are obviously correlated with the known earthquake population. These

FIGURE III-12
PROCEDURE FOR ASSOCIATING NEW OBSERVATIONS
WITH KNOWN CLUSTERS

ASSOCIATION OF DISCRIMINANT PATTERNS

- Establish statistical parameters of known populations ($M_j, \sigma_j^+, \sigma_j^-$; see Figure I-1)
 - $$z_{ij} = \frac{D_i - M_j}{\sigma_j}$$
 i^{th} unknown discriminant pattern normalized with j^{th} clustered population statistics
 - Find $\text{Min} \{|z_{ij}|\}$; most likely association by searching over j unknown event clusters.
- If $\text{Min} \{|z_{ij}|\} < \tau_j$; the event discriminant is associated with the j^{th} cluster.
- The association is unambiguous if no more than one cluster is below threshold τ_j .
- The association is ambiguous if more than one cluster is below τ_j (cross talk).

events are detected by the minimum deviation of their discriminant measures from established discriminant patterns. As previously described, a threshold is used to control the accumulation of errors in the parameter used to measure this minimum deviation from established discriminant patterns.

The association process is followed by a second stage of adaptive cluster analysis. The purpose here is to see if new clusters can be found which describe the remaining unidentified events.

If the discriminants prove to be effective, at least one cluster will contain explosions, and it will contain few, if any, earthquakes. Because of statistical variability, however, some explosions are expected to slip below the association thresholds to be classified either as unidentified events or to be falsely associated with an earthquake cluster.

Our experience indicates that the number of missed explosions corresponds closely to that expected from consideration of normal statistics. Therefore, a hypothesis that a single, central Asian explosion population exists cannot be rejected.

SECTION IV
ABILITY OF CLUSTER ANALYSIS TO SEPARATE
EARTHQUAKES AND EXPLOSIONS

The results produced by applying cluster analysis using discriminant patterns were summarized earlier (Section II, subsection E). This section includes a network summary of discrimination performance, the predicted operating characteristics of clustering based on threshold control assuming normal statistics, and cluster classification of events in the data base. It is notable that the predicted operating characteristics of the clustering technique are close to the observed network discrimination performance, and as such, there is no plausible basis for rejecting the hypothesis that a single explosion cluster exists.

Cluster analysis is an empirical procedure. The results are significant only if they are physically or operationally interpretable. The interpretation of the eight earthquake clusters is shown in Figure IV-1. The absence of cluster EQ-1 in the figure indicates that events formally associated with this cluster were passed into other clusters as a result of the iterative association process. Physically, cluster analysis identified and categorized normal, deep, and 'strange' explosion-like shallow events. The latter group exhibited strong, overshoot and high, apparent corner frequencies. High corner frequencies result from the presence of higher multipole moments in the source.

FIGURE IV-1
PHYSICAL AND OPERATIONAL INTERPRETATION OF THE
RESULTS OF THE EIGHT EARTHQUAKE CLUSTERS

INTERPRETATION OF CLUSTERING MODELS

- NORMAL EARTHQUAKES
 - EQ-5 Shallow depth, m_b of 4.1, few stations detected
 - EQ-2 Intermediate depth, median m_b of 4.5, few stations detected
 - EQ-6 Shallow depth, m_b of 4.9, many stations detected
 - EQ-8 Shallow depth, m_b of 4.9, many stations detected

- EARTHQUAKES ASSOCIATED WITH DEEP EVENTS
 - EQ-3 m_b of 4.5, few stations detected
 - EQ-7 m_b of 4.5, average number of stations detected

- REGIONAL EARTHQUAKE CLUSTER OF 'EXPLOSION LIKE' EARTHQUAKES
 - EQ-4 m_b of 4.7, many stations detected.

As used here, clustering of earthquakes showed a strong correlation with magnitude and with the number of stations detecting the events. This indicates that we had operational problems in the following areas:

- Proper magnitude scaling of the discriminants.
- Detecting and measuring weak signals.
- Proper determination of unbiased network magnitudes.

These problems were discussed thoroughly under Section III as methodology considerations.

The two aspects of gauging performance ... separation of explosions or defining clusters through the use of low-variance discriminant values ... are summarized in Figures IV-2 and IV-3. These figures clearly show the benefit of using many discriminants; they also display what could be considered as weaker discriminants (such as D_1 , D_2 , D_3 , and D_{11} , as is seen in Figure IV-2). However, even some of the weaker discriminants, such as D_1 and D_3 , seem to be useful in defining earthquake clusters with low variance, while even D_{11} helps to reduce the variance of the explosion population (as is seen in Figure IV-3). The inclusion of these weaker discriminants in the clustering process has the advantage of reducing the false alarm rate. Network performance, shown in Figure II-9, confirms that several false alarms were encountered in classifying the data as earthquakes or explosions. At this point, then, it is prudent to defer merging or eliminating redundant discriminants until the operational problems flagged by clustering are eliminated. Finally, note that the resolution of operational problems might alter the relative effectiveness of the discriminants used.

FIGURE IV-2
SEPARATION OF EXPLOSIONS

Discr.	EQ-1	EQ-2	EQ-3	EQ-4	EQ-5	EQ-6	EQ-7	EQ-8
D ₁	0	0	0					
D ₂		0	0	0				0
D ₃		0	0	0	0			
D ₄		●	●	●	●	0	●	
D ₅		0	●	0			0	0
D ₆	●	●	●	0	●	●	0	●
D ₇	0	●	0	0	●	0	0	0
D ₈	●	●	●	0	●	0	●	
D ₉	0			0	0	0	0	0
D ₁₀	●			0		●		●
D ₁₁								0
D ₁₂	●	0			0	0	0	
D ₁₃						●	●	
D ₁₄						●	●	0
D ₁₅								0
D ₁₆						●		●
D ₁₇								●
D ₁₈						●		0

0: OVER 50% EX'S SEPARATED FROM EQ GROUP
 ●: OVER 85% EX'S SEPARATED FROM EQ GROUP

FIGURE IV-3
POPULATION PINS

Discr.	EQ-1	EQ-2	EQ-3	EQ-4	EQ-5	EQ-6	EQ-7	EQ-8	EX-1
D ₁		0	●						
D ₂	0	0	0						
D ₃		●	●		●				
D ₄		0	●				0		
D ₅		0		0				0	
D ₆	●	●	0	●	0	0			
D ₇	0	●	0	●	0				
D ₈	●	●			0				
D ₉	0		0	0	0				
D ₁₀	0					●			
D ₁₁									0
D ₁₂	0	0							
D ₁₃						0			
D ₁₄									
D ₁₅									●
D ₁₆									
D ₁₇						0			
D ₁₈									

0 < 25% OF DISCRIMINANT RANGE
● < 12.5% OF DISCRIMINANT RANGE

SECTION V CONCLUSIONS

Our major contribution to the Event Identification Experiment was the development and demonstration of a systematic, objective, and robust procedure for performing event identification. This procedure allows us to rapidly implement, test, and improve effective event discrimination procedures. Specifically, the procedure used accurately classifies events as earthquakes or as explosions by means of their 'like' discriminant patterns. The association of various events with one another is based on an empirical cluster analysis technique. Using this technique, we not only demonstrated that events can be accurately classified, but also, that magnitude scaling problems and other operational problems, as well, can be identified with speed and certainty. Furthermore, the systematic clustering procedure used allowed us to correct the main operational problem of magnitude scaling, to process the properly scaled discriminants, and to obtain corrected results within a short period of time (a matter of a few days).

Using discriminants corrected for magnitude scaling problems, we found that we could identify events using only a single earthquake cluster and a single explosion cluster. Without proper magnitude scaling, on the other hand, eight earthquake clusters were required to produce this same result.

Another more subtle aspect of the results obtained was that by properly scaling the discriminants, their relative effectiveness was dramatically changed. The latter result demonstrated the importance of insuring that all operational problems are resolved before prejudging the efficacy of the individual discriminants.

The Event Identification Experiment was a significant learning experience. In Figure V-1, we list eleven factors which strongly influenced our performance. Considerable improvement in event identification performance should be obtained by implementing automated quality control into the editing process and by implementing advanced signal analysis procedures for minimizing the influence of seismic noise.

The use of cluster analysis to identify events by their physical source characteristics and to identify operational difficulties which prevent event classification is a new approach to event identification by means of multiple discriminants. The technique is basically a statistical learning process which gives the scientist a capability to group explosion events without requiring any prior knowledge of explosion or earthquake discriminant patterns. That is, the technique is based only on observing consistent repeatable discriminant patterns. Other analysis means, such as physical modeling and extended signal analysis, can subsequently be used to identify clusters of anomalous or unusual events as probably explosions. This statistical learning process is summarized in Figure V-2.

FIGURE V-1
FACTORS INFLUENCING PERFORMANCE

1. QUALITY CONTROL
2. SIMPLE STANDARD AUTOMATED PROCEDURES
3. EARTHQUAKE TRAINING
4. PHYSICAL VALIDITY OF DISCRIMINANTS
5. STATISTICAL LEARNING
6. ADAPTIVE DISCRIMINATION (DETECT NEW CLUSTERS)
7. DISCRIMINANT PATTERN ASSOCIATION (CLUSTERING)
8. NOISE MINIMIZATION
9. SUFFICIENT DATA
10. REDUNDANCY
11. STABILITY TESTING

FIGURE V-2
CLASSIFICATION OF EVENTS AS EARTHQUAKES OR EXPLOSIONS

STATISTICAL LEARNING PROCESS

- TRAIN MULTIPLE DISCRIMINANTS ON EARTHQUAKES
- IF POSSIBLE, ASSOCIATE EVENTS WITH ESTABLISHED EARTHQUAKE OR EXPLOSION CLUSTERS
- GROUP OTHER EVENTS BY ADAPTIVE CLUSTERING
- NEW CLUSTERS ARE IDENTIFIED AS EARTHQUAKES OR EXPLOSIONS BASED ON:
 - PHYSICAL CHARACTERISTICS
 - ASSOCIATION WITH KNOWN EARTHQUAKES OR EXPLOSIONS (BASED ON NON-SEISMIC INFORMATION).

As noted above, several operational problems were identified as a result of applying cluster analysis and of quality control checking of the waveform editing process. These operational problems are summarized below:

- Eliminate large timing errors, and, consequently, large magnitude measurement errors.
- Use advanced signal analysis techniques to minimize the influence of seismic noise (i.e., to improve the signal-to-noise ratio of weak signals).
- Apply a high-resolution filtering technique in the measurement of band-limited magnitudes. To do otherwise produces bias in estimates of the variable frequency magnitudes.
- Re-examine and modify the network magnitude averaging technique currently employed. Presently, the method used grossly underestimates the magnitudes of events having few detections.
- Apply more effective discriminants and eliminate those discriminants which are shown to be ineffective. However, this should only be done after eliminating obvious operational problems.
- Use synthetics as an alternative source of data for cluster analysis.
- Consider the application of discriminants on the basis of seismic region. This obviously requires a much larger data base in order to sample all seismically active regions as well as to sample large aseismic, plate regions.

In sum, our approach to event identification is to assemble a set of effective discriminants and to associate and identify events by their 'like' discriminant patterns (clusters). The underlying philosophy to this approach is summarized in Figure V-3; what we have learned in our first attempt to apply cluster analysis is summarized in Figure V-4.

FIGURE V-3
OUR PHILOSOPHY OF EVENT IDENTIFICATION

- BOTH EARTHQUAKES AND EXPLOSIONS ARE COMPLEX PHYSICAL PROCESSES REQUIRING THE USE OF MULTIPLE DISCRIMINANTS FOR UNIQUE EVENT IDENTIFICATION
- SIMILAR SOURCE MECHANISMS SHOULD YIELD SIMILAR DISCRIMINANT PATTERNS
- THE DISCRIMINANT SET WILL EVOLVE TO ENCOMPASS ALL TYPES OF EARTHQUAKES AND EXPLOSIONS
- STABLE EVENT CLUSTERS DETECTED EMPIRICALLY MUST BE PHYSICALLY OR OPERATIONALLY CHARACTERIZED, OR THEY MUST BE DISCARDED
- DISCRIMINANTS SHOULD BE GENERALIZED AND IMPROVED UPON BY PHYSICAL SOURCE STUDIES
- PRACTICAL IDENTIFICATION PROCEDURES WHICH ARE DEVELOPED SHOULD BE IMPLEMENTABLE ON A REAL-TIME SYSTEM
- A SYSTEMS APPROACH WILL BE APPLIED TO IDENTIFICATION IN ORDER TO SPEED THE LEARNING PROCESS, TO PROVIDE FOR FLEXIBLE ANALYSIS, AND TO EASE DATABASE MAINTENANCE REQUIREMENTS.

FIGURE V-4
WHAT WE HAVE LEARNED

- A SYSTEM APPROACH TO DISCRIMINATION FACILITATES
 - MODIFICATION OF PROCEDURES
 - TURNAROUND ON LARGE DATA SETS
 - LEARNING
 - QUALITY CONTROL

- BY TRAINING ON EARTHQUAKES WITH CLUSTER ANALYSIS, WE LEARNED THAT
 - MAGNITUDE SCALING IS OUR MOST SERIOUS PROBLEM
 - NOISE (i.e., lack of detection) IS ALSO A SERIOUS PROBLEM

- BY USING CLUSTER ANALYSIS OF EVENTS OBSERVED AT DIFFERENT STATIONS, WE LEARNED THAT THE
 - MAGNITUDE-DISTANCE SCALING USED APPEARS VALID
 - CALIBRATION OF ABSOLUTE MAGNITUDES APPEARS VALID
 - TREATMENT OF NOISE IN NETWORK AVERAGING IS A SERIOUS PROBLEM

- MULTIVARIATE DISCRIMINATION IS NOT FEASIBLE UNTIL
 - INDIVIDUAL DISCRIMINANTS ARE PROPERLY SCALED
 - AT LEAST ONE STABLE CLUSTER IS OBTAINED FOR EARTHQUAKES AND EXPLOSIONS
 - DISCRIMINANTS AND CLUSTERS MUST BE PHYSICALLY WELL BASED.

SECTION VI
REFERENCES

- Anglin, F. M., 1971; Discrimination of Earthquakes and Explosions using Short-Period Array Data, Nature, Vol. 233, 51-52.
- Bache, T. C., J. T. Cherry, and J. M. Savino, 1974; Application of Advanced Methods for Identification and Detection of Nuclear Explosions from the Asian Continent, Systems, Science and Software Semi-Annual Report No. SSS-2-75-2483, Contract Number F44620-74-C-0063, La Jolla, CA.
- Bell, A. G. R., 1978; Application of Two Multivariate Classification Techniques to the Problem of Seismic Discrimination, M.S. Thesis, The Pennsylvania State University, University Park, PA.
- Booker, A., and W. Mitronovas, 1964; Application of Statistical Discrimination to Classify Seismic Events, Bull. Seismol. Soc. Am., 54, 961-971.
- Claerbout, J. F., 1976; Fundamentals of Geophysical Data Processing, McGraw Hill, New York, NY.
- Dietz, D. L., and R. L. Sax, 1978; Relationships Between Noise and m_b Bias Applied to Seismic Station Site Selection, Texas Instruments Report No. ALEX(01)-TR-77-12, AFTAC Contract Number F08606-77-C-0004, Texas Instruments Incorporated, Dallas, TX.

- Evernden, J. F., 1967; Magnitude Determination of Regional and Near-Regional Distances in the United States, Bull. Seismol. Soc. Am., 57, 591-639.
- Evernden, J. F., and W. M. Kohler, 1976; Bias in Estimates of m_b at Small Magnitudes, Bull. Seismol. Soc. Am., 66, 1887-1904.
- Fitch, T. J., M. W. Shields, and R. E. Needham, 1978; Comparison of Crustal Phase Magnitudes for Explosions and Earthquakes, Seismic Discrimination Semi-Annual Technical Summary, Lincoln Laboratory, MIT, Lexington, MA.
- Fix, J. E., J. G. Swanson, and W. D. Ballard, 1973; Study of Selected World-Wide Seismograph Network Stations, Seismic Array Analysis Center, Report No. 11, Teledyne Geotech, Garland, TX.
- Hair, G. D., J. H. Funk, and Research Staff, 1964; Noise Study, Special Report No. X, Texas Instruments Incorporated, Dallas, TX.
- Hsiao, H. Y. A., 1978; Application of a Combined Source Model for Seismic Discrimination, Technical Report No. 21, Texas Instruments Report No. ALEX(01)-TR-78-09, AFTAC Contract Number F08606-77-C-0004, Texas Instruments Incorporated, Dallas, TX.
- Liebermann, R. C., and P. W. Pomeroy, 1969; Relative Excitation of Surface Waves by Earthquakes and Underground Explosions, J. Geophys. Res., 74, 1575-1590.
- Marshall, P. D., and P. W. Basham, 1972; Discrimination Between Earthquakes and Underground Explosions Employing an Improved m_b Scale, Geophys. J. R. Astr. Soc., 28, 431-458.

- North, R. G., 1977; Station Magnitude Bias - Its Determination, Causes, and Effects, Technical Note 1977-24, Lincoln Laboratory, MIT, Lexington, MA.
- Nuttli, O. W., 1973; Seismic Wave Attenuation and Magnitude Relations for Eastern North America, J. Geophys. Res., 78, 876-885.
- Ringdal, F., 1974; Estimation of Seismic Detection Thresholds, Technical Report No. 2, Texas Instruments Report No. ALEX(01)-TR-74-02, AFTAC Contract Number F08606-74-C-0033, Texas Instruments Incorporated, Dallas, TX.
- Ringdal, F., 1975; Maximum Likelihood Estimation of Seismic Event Magnitudes from Network Data, Technical Report No. 1, Texas Instruments Report No. ALEX(01)-TR-75-01, AFTAC Contract Number F08606-75-C-0029, Texas Instruments Incorporated, Dallas, TX.
- Rivers, W. D., 1979; Effect of Tectonic Strain Release on Surface Wave Magnitudes, Talk presented at VELA Seismological Center Research Review, Alexandria, VA.
- Sax, R. L., 1976; Design, Simulated Operation and Evaluation of a Short-Period Seismic Discrimination Processor in the Context of a World-Wide Seismic Surveillance System, Technical Report No. 9, Texas Instruments Report No. ALEX(01)-TR-76-09, AFTAC Contract Number F08606-76-C-0011, Texas Instruments Incorporated, Dallas, TX.
- Sax, R. L., and Technical Staff, 1978; Event Identification - Applications to Area of Interest Events, Technical Report No. 20, Texas Instruments Report No. ALEX(01)-TR-78-08, AFTAC Contract Number F08606-77-C-0004, Texas Instruments Incorporated, Dallas, TX.

Sax, R. L., A. G. R. Bell, and D. L. Dietz, 1979; (S) Event Identification Experiment: Combined Priority I/Priority II Data Sets (U), Technical Report No. 7, ENSCO Report No. SAR(01)-TR-79-07, AFTAC Contract Number F08606-79-C-0014, ENSCO Incorporated, Alexandria, VA.

Strauss, A. C., 1978; Application of Ringdal's Method to Unbiased Measurement of the M_s - m_b Relationship, Technical Report No. 15, Texas Instruments Report No. ALEX(01)-TR-78-03, AFTAC Contract Number F08606-77-C-0004, Texas Instruments Incorporated, Dallas, TX.

Unger, R., 1978; Automatic Detection, Timing and Preliminary Discrimination of Seismic Signals with the Instantaneous Amplitude, Phase, and Frequency, Technical Report No. 4, Texas Instruments Report No. ALEX(01)-TR-77-04, AFTAC Contract Number F08606-77-C-0004, Texas Instruments Incorporated, Dallas, TX.

Veith, K. F., and G. E. Clawson, 1972; Magnitude from Short-Period P-Wave Data, Bull. Seismol. Soc. Am., 62, 435-452.

APPENDIX A
THE AUTOMATIC EDIT DETECTOR

The detector designed by Unger (1978) operates on time sequences of instantaneous amplitude and phase measurements. The detection concept is based on a simplified model of a random phase, modulated noise component which is vectorially added to a fixed signal component as follows:

$$s(t) = S(t)\cos(2\pi f_0 t + \phi_s(t)) \quad (\tau_1 < t < \tau_2)$$

$$n(t) = N(t)\cos(2\pi f_0 t + \phi_n(t)),$$

where τ_1 and τ_2 define a time gate containing the signal, and $S(t)$ and $N(t)$ are instantaneous envelope traces of the seismic signal and noise, respectively. The envelope modulation components are slowly varying compared to the phase modulated component in the above waveform representations. Also, the instantaneous phase $\phi_n(t)$ is presumed to vary rapidly, randomly, and uniformly between 0 and 2π with respect to the signal phase $\phi_s(t)$.

A simplified model representing interfering signals and noise was obtained by adding $s(t)$ and $n(t)$. Further, $S(t)$ and $N(t)$ are approximated by fixed nominal values S and N in the signal window between T_1 and T_2 ; $\phi_s(t)$ is arbitrarily set to zero. Modulation of the signal is modeled by random phase changes of the interfering noise component $\Delta\phi(t)$.

This leads to the following simplified model for additive signal and noise:

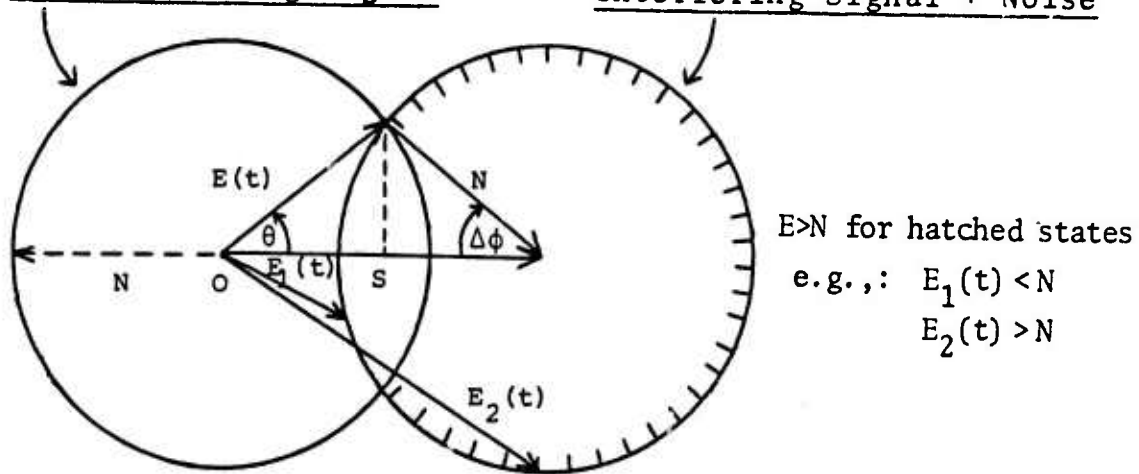
$$\begin{aligned} x(t) \equiv s(t)+n(t) &= E(t)\cos\theta(t) = S\cos(2\pi f_0 t) \\ &+ N\cos(2\pi f_0 t+\Delta\phi(t)), \end{aligned}$$

where $E(t)$ is the envelope. Phase modulations, $\Delta\phi(t)$, of noise are equally likely to occur between 0 and 2π . By geometrical considerations, this procedure provides an analytical basis for estimating the probability that the envelope $E(t)$ of interfering signal and noise in the signal gate T_1 to T_2 exceeds noise. This concept for timing signals by counting excessions of noise in a leading time gate is shown graphically in Figure A-1. For implementation purposes, noise N would be gauged from instantaneous envelope measurements of noise preceding a moving-gate, signal time window.

The results derived in Figure A-1 indicate the following:

- For signals less than 6 dB over noise, peaks of $P(E(t)>N)$ correspond to $S/N=\max<2$. Therefore, the algorithm is a maximum likelihood timer of weak signals, and it is independent of the statistical distribution of the noise.
- For signals 6 dB over noise, $P(E(t)>N)=1.0$, i.e., always exceeds noise.
- First encountered occurrences of maximum peak above a threshold or saturated unity values of $P(E(t)>N)$ are taken to indicate the onset time of a signal.

Vectors from origin, O, represent possible states of
Noise Preceding Signal Interfering Signal + Noise



E represents the envelope of interfering signal + Noise;
 N, noise; and S, signal.

$$\cos \Delta\phi = \frac{S}{2N} \qquad \Delta\phi = \cos^{-1} \frac{S}{2N}$$

Since $\Delta\phi$ is equally likely to occur between 0 and π , the fraction of interfering signal and noise exceeding noise is shown for the model by the hatched line. The probability of $E(t)$ exceeding the noise level, N, is given by:

$$P(E(t) > N) = \begin{cases} 1 - \frac{1}{\pi} \cos^{-1} \left(\frac{S}{2N} \right) & (0 < \frac{S}{N} \leq 2) \\ 1 & \frac{S}{N} > 2 \end{cases} \quad (1)$$

Even for an infinitesimal signal, $E(t)$ exceeds noise half the time. $P(E(t) > N)$ ranges from 0.5 to 1.0 and is 1.0 for $\frac{S}{N} > 2$.

FIGURE A-1
 PROBABILITY OF MEASURED ENVELOPE EXCEEDING NOISE
 AS A ROBUST DETECTION CONCEPT FOR TIMING WEAK SIGNALS

These results formed the concept of a detector which optimally times the arrival of short-period P waves. The detector gauges $P(E(t) > N)$ by measuring the fraction of excessions of N by $E(t)$ in a leading four-second time window. This is potentially a robust algorithm for detecting signal onset times. For example, estimates of N by the median of noise preceding a signal are insensitive to large fluctuations due to non-stationary noise or signals, or due to system noise. Ramps characterizing the onset of emergent signals will not greatly affect this estimate of N until at least half of the noise gate overlaps the signal. Counting the number of $E(t) > N$ states in the signal window is also a robust calculation, and is similarly insensitive to spikes, 'glitches', and to other sources of large amplitude errors.

Analyst comparison tests of the automatic timing detector given by Unger (1978) indicated that nearly half of the events examined were timed with no apparent error. All but a few of the 28 events were timed with errors less than 0.5 seconds. Unger observed that the detector had a slight tendency to pick arrival times late by ignoring small peaks at the beginning of the signal. This tendency was corrected by detecting the first envelope peak, measuring the period of the peak, and backing up three-quarters of a cycle to time more accurately the first motion of the signal.

Experience gained from using Unger's detector in the Event Identification Experiment indicated that the detector produced a negligible number of false alarms. Almost all detected signals were accurately timed, including cases with barely visible signals. A problem was encountered with missed

signals. In most cases these were either gradually emergent signals, or short, impulsive signals of duration much less than the leading four-second time gate. There are many ways these deficiencies can be corrected; e.g., using a variable-length time gate, employing median in place of maximum estimates of noise in the time gate preceding the signal window, and by parallel operation of a power detector which is designed to capture large emergent signals of short duration. In a few cases, large, easily detected signals of at least four seconds duration were missed. This problem could have also been avoided by changing the algorithm from the presently used maximum noise peaks to median noise preceding the signal in order to prevent short intervals of large noise or spikes from inadvertently shutting off the detector.

Another problem observed in automatically timing signals stemmed from (apparent) multiple event arrivals. The short-period edit process involves timing events of approximately known origin time, distance, and magnitude. The problem of correctly associating one of several event or phase arrivals with a known event can be accomplished as follows:

- List all apparent phase arrival times detected on the seismic record.
- Compute magnitude and time residuals associated with each phase arrival time.
- Select the P phase most likely to be associated with the event as that which minimizes the apparent travel-time and magnitude errors.

For the event identification data base, this association process is facilitated by a statistical summary of magnitude

and time residuals, along with the corresponding standard deviations for these parameters.

APPENDIX B
VARIABLE FREQUENCY MAGNITUDE MEASUREMENT BY A
FIXED BANK OF SHORT-PERIOD AND
LONG-PERIOD BANDPASS FILTERS

A. OPTIMUM DESIGN OF BANDPASS FILTERS

Gaussian bandpass filters were optimized to measure frequency-dependent magnitudes. A mathematical analysis of the filtering process is shown in Figure B-1. The envelope of a Gaussian-filtered impulsive signal is $\exp[-\pi(\Delta f)^2 t^2]$. For two, equal-amplitude signals separated by a time interval Δt , the envelope trace $\ell(t)$ is given by:

$$\ell(t) = \exp-\pi(\Delta f)^2 \left(t - \frac{\Delta t}{2}\right)^2 + \exp-\pi(\Delta f)^2 \left(t + \frac{\Delta t}{2}\right)^2,$$

where Δt is the separation of envelope peaks in the time domain and Δf is the filter bandwidth. Consider the envelope trace for the case where $\Delta f \cdot \Delta t = 1$. Midway between the two signals, at $t=0$, $\ell(0) < 0.9$; at $t = \pm \Delta t/2$, $\ell > 1.0$. On this basis the peaks are distinguishable if $\Delta f \cdot \Delta t \geq 1$. If time-domain peaks occur in a much smaller time interval than $\Delta t = 1/\Delta f$, they are integrated into a larger single peak which biases and increases the variance of magnitude measurements. This lower limit of Δt for resolving the two signals as envelope peaks is minimized by the use of Gaussian filters.

The main design problem in the use of filters is to provide sufficient frequency resolution consistent with an

FIGURE B-1
 MATHEMATICAL DERIVATION OF FILTERING PROCESS

GAUSSIAN FILTERS

- The following are symbol definitions

	frequency-domain	time-domain
Seismic Data	D(f)	d(f)
Gaussian Filter	B(f)	b(f)
Filtered Data	F(f)	f(f).

- The spectrum of the Gaussian filter is given as follows

$$B(f) = \exp - \pi \left[\frac{f - f_0}{\Delta f} \right]^2 \quad (1)$$

where f = frequency

f_0 = center frequency of filter

Δf = full bandwidth of filter.

- The impulse response is obtained by Fourier transformation

$$b(t) = \Delta f \{ \exp - \pi \Delta f^2 t^2 \} \cos 2\pi f_0 t. \quad (2)$$

- The spectral and time-domain state of the filtered data is given by the product of the spectrum;

$$F(f) = B(f)D(f)$$

$$f(t) = \int_{-\infty}^{+\infty} F(f) \exp i2\pi ft \, df;$$

or by convolution of the time-domain filter with the data

$$f(t) = \int_{-\infty}^{+\infty} b(t-t_0) dt_0.$$

adequate resolution of the envelope peaks of signals occurring in a signal time window. In the Event Identification Experiment, this tradeoff was evaluated empirically using variable bandwidth measurements of the magnitude of P-wave signals.

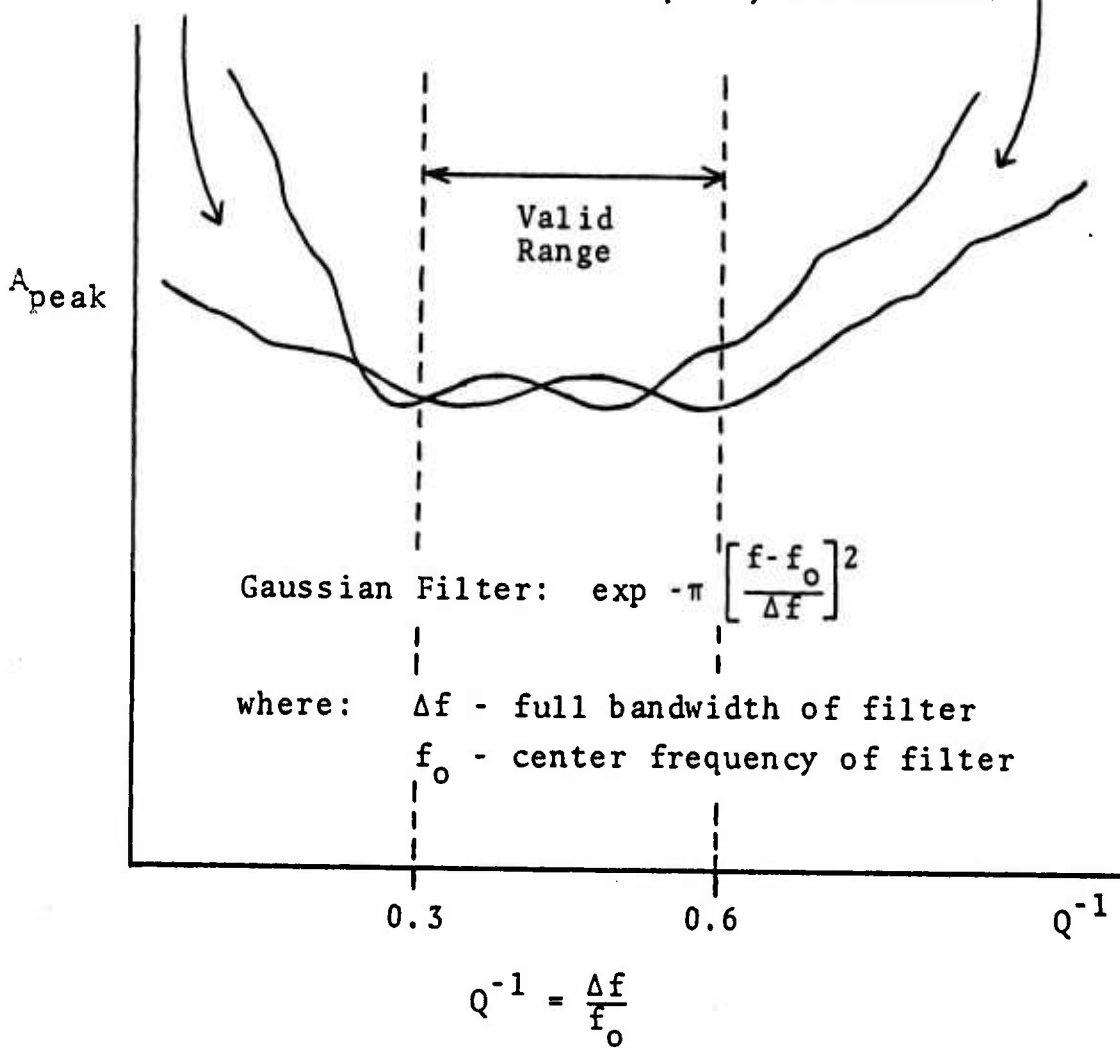
Inspection of equation (2) in Figure B-1 indicates that for a filtered unit-amplitude impulsive signal, the envelope peak is equal to the bandwidth, Δf . This indicates that peak envelope measurements of signals are consistently related to the magnitude of a broadband input signal by dividing these measurements by the full bandwidth of the filter, Δf . However, P-wave signals are not impulses; they are, instead, complex waveforms which include a random coda component. The validity of normalizing filtered signal magnitudes, then, by dividing peak amplitude measurements by the filter bandwidth, was tested experimentally. The results of these tests are shown schematically in Figure B-2.

In all cases tested, covering a wide range of short-period frequencies from 0.3 to 3.0 Hz, normalization by the filter bandwidth provided accurate and consistent signal magnitudes provided that the Q^{-1} (as defined in Figure B-2) of the filter is constrained to lie between 0.3 and 0.6. In fact, Q^{-1} of 0.45 appeared to be optimum, and this value was used to design all of the short-period filters used in the Event Identification Experiment.

The result of testing long-period magnitude measurements, which were filtered at frequencies from 0.02 to 1.0 Hz, was quite different. The long-period data that were

Interference of multipath and coda noise peaks due to lack of time resolution.

Leakage of spectral noise and signal peaks due to lack of frequency resolution.



l_{peak} envelope peak in signal window

Normalization: $A_{\text{peak}} = l_{\text{peak}} / \Delta f$

FIGURE B-2
 NORMALIZATION OF SHORT-PERIOD FILTERED
 MAGNITUDE MEASUREMENTS

tested indicated that filtered amplitude peaks were consistently less dependent on Q^{-1} and on filtered bandwidth. Thus, a quasi-sinusoidal signal model, having an effective bandwidth which is equal to, or less than, that of the signal, appeared to be the most appropriate model for long-period magnitude measurements. For example, a signal having its peak amplitude at 25 seconds period yielded approximately the same magnitude for different filters with Q^{-1} values ranging from 0.3 to 0.6. This result was not unexpected for dispersed sinusoidal signals. Consequently, we measured the filtered, long-period magnitudes based on the assumption of a quasi-sinusoidal signal input having bandwidth less than that of the filter. For this purpose, a fixed bandwidth of 0.01 Hz was used for long-period filter magnitude measurements. These data were not normalized by dividing by Δf , as was the case for the short-period filtered magnitude measurements.

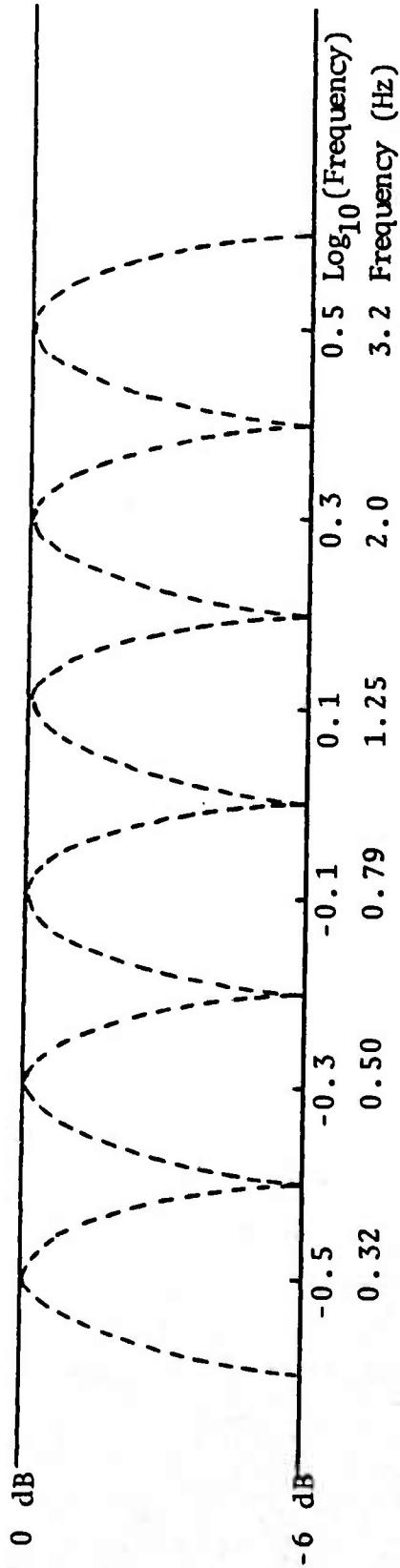
Figure B-2 schematically illustrates the bias and variance of filtered magnitude measurements which fell outside of the empirically determined, acceptable range of filter bandwidth. If the bandwidth is too small, time peaks are integrated, and produce a large positive bias of the magnitude. The variance of the magnitude measurements is also increased since effects produced by multipath signals and coda vary from station to station. If the bandwidth is too large, positive bias and increased variance of filtered magnitude measurements are produced by leakage from spectral peaks associated with the noise or the signal.

This empirical approach to optimizing the filtered magnitude measurements was considered necessary because of the speculative nature of any theoretical treatment of the problem (due, in large part to the complexity and diversity of seismic signals and noise). For a more complete evaluation of filters, additional data, covering different source and receiver tectonic environments, and different source mechanisms (e.g., shallow and deep earthquakes, and explosion sources) need to be examined.

B. SAMPLING OF SPECTRAL MAGNITUDES AND MINIMIZATION OF RADIATION PATTERN EFFECTS

Our initial, simplified approach to the discrimination problem was to model event-filtered magnitudes as a set of constants which characterize the source type. These magnitudes are estimated from signal and noise measurements through application of the maximum likelihood criteria. In the preceding section on filter optimization, we noted that empirically, a narrow range of Q filters was found to be optimum for measuring short-period magnitudes. We further noted that these optimum filters were rather broadband, in nature, with Qs ranging from 1.7 to 3.4. Further, from design optimization considerations based on time-frequency sampling analysis, short-period magnitudes are measured at logarithmically spaced center frequencies, as is shown in Figure B-3. For filtered, long-period magnitude measurements, filters were centered uniformly along the frequency axis, with a bandwidth of 0.01 Hz.

SHORT-PERIOD FILTERS



LONG-PERIOD FILTERS

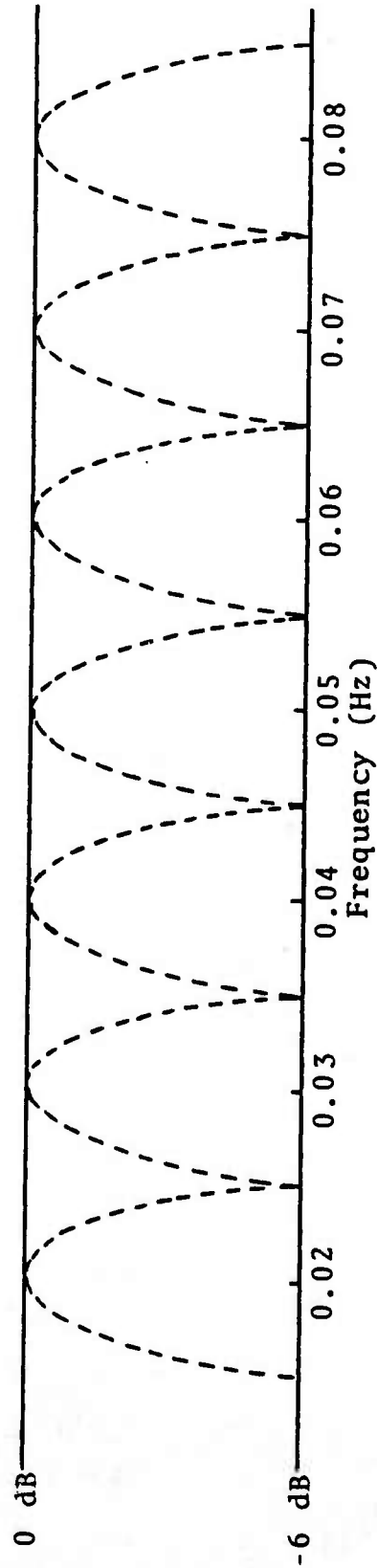


FIGURE B-3
SCHEMATIC REPRESENTATION OF SHORT-PERIOD AND LONG-PERIOD FILTER COMBS

In using fixed-magnitude levels as basic information from which to compute event discriminants, a source of errors are holes in the spectrum which occur at stations lying along a node of the source radiation pattern, (holes are in the spectrum because of source dynamics). These effects are minimized by broadband frequency sampling provided by the short-period filters. In addition to covering spectral holes of narrow bandwidth, there is sufficient time resolution to sample several independent degrees of freedom in the signal window by means of coda backscattering and multipath propagation of energy from rays not oriented along the node. Thus, use of low-Q filters should tend to smooth complexities of source geometry, and should provide better correspondence to a simplified model of fixed, spectral-magnitude levels characterizing different types of sources. Observations of earthquake source spectra for several event-station pairs, after correcting for absorption, correspond closely to simple signal models with (roughly) flat spectra at low frequencies, and uniform roll-offs above the apparent corner frequency.

C. ERROR ANALYSIS OF SPECTRAL LEAKAGE

A filtered signal amplitude spectrum is equal to the product of the signal and filter amplitude spectra. Since magnitude measurements are derived from peak-amplitude measurements, frequency variability of spectral peaks is a significant source of magnitude measurement error; this is especially true for events for which the signal spectrum changes rapidly with frequency. If the peak frequency of the filtered signal spectrum occurs outside an acceptance band

for valid magnitude measurement (e.g., within a frequency interval where the filter response is less than 3 dB down), the magnitude measurement is considered to be invalid. Such erroneous magnitude measurements are considered to result from spectral leakage from signal or noise signatures too far removed in frequency to be representative of the desired frequency band. The main effect of spectral leakage is to cause a positive bias to filtered magnitude measurements; then, too, for each source type, spectral leakage increases the variance from event-to-event and from station-to-station. Event-to-event variations occur primarily at high frequencies, and are evidenced by variable corner frequencies and variable roll-off characteristics above the corner frequency. Station-to-station variations occur mainly at high frequencies, and are probably associated with the variable absorption of energy along the propagation path.

The significance of the spectral leakage effect was evaluated numerically for several plausible earth models. A simple model was used to evaluate the significance of errors caused by spectral leakage. Signal parameters affecting spectral leakage are:

- Absorption
- Corner frequency
- High frequency spectral roll-off
- Filter response characteristics.

The roll-off of a source model's amplitude with frequency is expected to be close to zero below the corner frequency. Above the corner frequency, the roll-off is proportional to

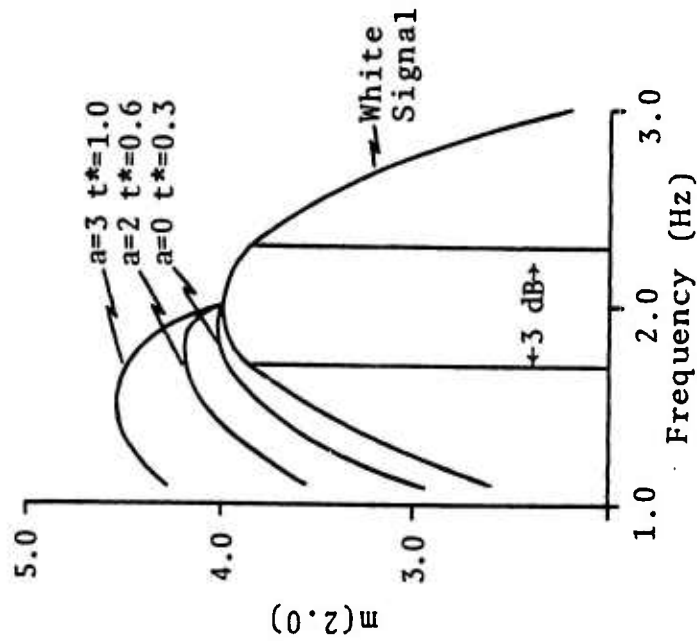
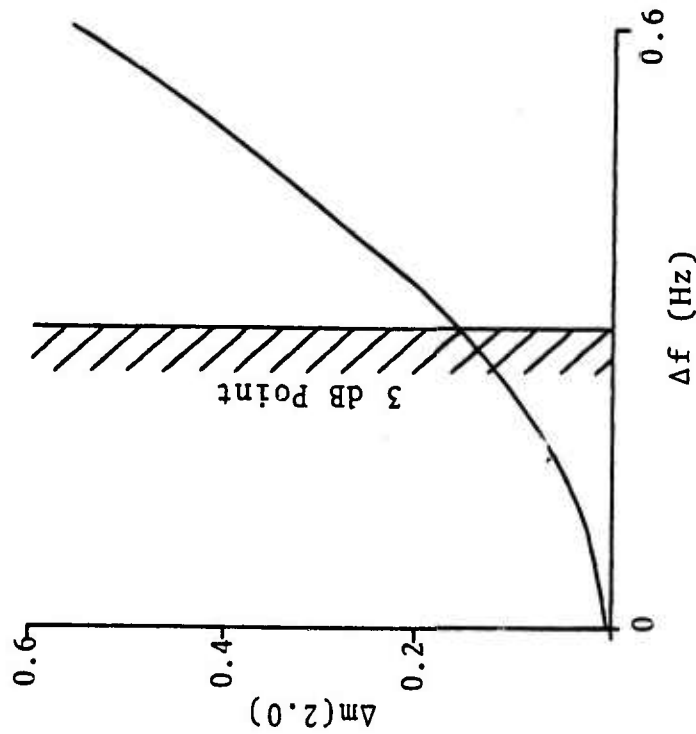
f^{-a} , where the integer a varies between one and three. Absorption of short-period P waves is approximated by a t^* model as $\exp[-\pi(t^*f)]$.

The following example illustrates the effect on frequency-dependent magnitude caused by variations in t^* . A very low absorption path (perhaps too low) is represented by $t^*=0.3$; nominal absorption, by $t^*=0.6$; and high absorption, by $t^*=1.0$. These values are considered representative of different absorption paths. The magnitude and frequency deviations caused by these effects, therefore, are assumed to typify the variability of magnitude measurements one would observe. The results of the frequency-dependent- t^* study are shown in Figure B-4 for a filter centered at 2.0 Hz, and for an optimum Q^{-1} of 0.45 (see Figure B-2). The results indicate that for a typical earth model, a leakage problem exists when one attempts to measure high frequency magnitudes above the corner frequency. The positive bias of magnitude measurements made at 2 Hz varies between 0 and 0.6 m_b units depending on which earth model is assumed for a particular event-station path.

A stability problem also exists in measuring the magnitudes of signals with peak frequencies occurring in the side-band of the Gaussian filter. Because of multipath arrivals and scattering through a heterogeneous earth, instantaneous frequency fluctuations are normally observed in the 10-second signal window. The effect of the filter response of such fluctuations occurring in signals with the dominant frequency in the side-band of the filter is to increase greatly the variance of the magnitude measurements. For example, for a

SIDEBAND LEAKAGE ERROR OF GAUSSIAN FILTERS

Magnitude Measurement Error



$$\text{Model: } A(f) = \frac{\text{EXP}(-\pi t^* f)}{1 + (\frac{f}{f_c})^a} + \text{EXP}(\frac{f-f_0}{0.5})^2$$

Signal and Absorption Model

Gaussian Filter

FIGURE B-4

VARIABILITY OF FILTERED MAGNITUDE MEASUREMENTS

signal spectrum roll-off proportional to f^{-3} , an absorption t^* of 1.0, and a frequency uncertainty of ± 0.15 Hz, the magnitude uncertainty is about $\pm 0.6 m_b$ units. On the other hand, for a flat signal spectrum and a t^* of 0.3, the magnitude uncertainty produced by the filter side-band 'amplification' is only $\pm 0.1 m_b$ units. Thus, the nominal magnitude measurement errors shown as a function frequency error in Figure B-4 have (approximately) equal, large uncertainty limits produced by normally observed peak-frequency fluctuations. A consequence of this variance of the magnitude bias is that there is probably no reliable means by which to correct such magnitude errors by sensing the frequency error associated with the measured magnitude. For example, in Figure B-4, if the 2 Hz filter output is sensed to be 1.4 Hz, a correction of $-0.6 m_b$ units is indicated. However, the uncertainty associated with this correction is expected to be about $\pm 0.6 m_b$ units. Thus, correcting magnitudes using frequency measurements is probably not adequate. Some other action must be taken to cope with the positive magnitude bias and the variance problem associated with spectral leakage.

D. PRESENT METHOD OF FILTERED MAGNITUDE MEASUREMENT TO MINIMIZE SPECTRAL LEAKAGE ERRORS

For teleseismic events ($\Delta > 20^\circ$), filtered magnitudes are calculated by using Veith and Clawson (1972) P-factors. Regional phase magnitudes are calculated from relationships given by Evernden (1967) for Pn; Fitch, et al. (1978) for Sn; and Nuttli (1973) for Lg.

After the data trace is filtered, the instantaneous signal envelope and frequency are generated by complex signal analysis. A filtered waveform $x(t)$ is taken as the real part of the signal. The imaginary part of the signal, $y(t)$, is obtained by means of a Hilbert transform, which shifts the phase of each spectral component of $x(t)$ by $\pi/2$. The complex signal waveform so constructed is given by $z(t)=x(t)+iy(t)$. Instantaneous measurements of signal amplitudes and frequencies are obtained by the method described in Figure B-5.

The following method is now applied to avoid large magnitude errors caused by spectral leakage. The magnitudes of filtered signals are determined from peak amplitudes in a 10-second signal time window. Each observed instantaneous amplitude $\ell(t)$ is associated with an instantaneous frequency measurement $f(t)$. If $|f(t)-f_0|$ (where f_0 is the center frequency) exceeds a threshold of δf , then $\ell(t)$ is considered to derive from leakage, and so, $\ell(t)$ is weighted zero (0). The threshold criteria presently used for this frequency test is to reject filtered signals of the dominant frequency shift δf where the filter response is more than 6 dB down. If the frequency deviation of the filtered signal is equal to, or less than, δf , the envelope measurement $\ell(t)$ is considered valid. The maximum value of valid amplitude measurements in the 10-second signal window is used to compute the magnitude of the signal. This concept of a frequency acceptance band is illustrated in Figure B-4; here, a 3 dB down criterion is applied to validate signal amplitude measurements.

FIGURE B-5
 ENVELOPE AND PHASE MODULATED SIGNALS

COMPLEX SIGNAL ANALYSIS

$X(t)$ is defined as the real measured signal waveform. The spectrum of $X(t)$ is

$$X(f) = \int_{-\infty}^{\infty} X(t) \exp i 2 \pi f t d t = C(f) + i S(f).$$

The spectrum of the imaginary signal component, constructed as $iX(f) = -S(f) + iC(f)$, is transformed to the time domain as $y(t)$.

The complex signal in rectangular and polar coordinates is

$$z(t) = X(t) + iy(t) = \rho(t) [\cos \phi(t) + i \sin \phi(t)] . \quad (1)$$

The time-varying envelope as the modulus of $z(t)$ is

$$\rho(t) = |z(t)| = (x(t)^2 + y(t)^2)^{1/2}. \quad (2)$$

The time-varying phase angle of $z(t)$ is

$$\phi(t) = \tan^{-1} [y(t)/X(t)]. \quad (3)$$

The time-varying dominant frequency component is

$$f(t) = \frac{1}{2\pi} \frac{d\phi(t)}{dt} = \frac{1}{2\pi} \frac{x(t) \frac{dy(t)}{dt} - y(t) \frac{dx(t)}{dt}}{\rho^2(t)} \quad (4)$$